Evolution, 55(11), 2001, pp. 2215–2235

TRENDS IN THE EVOLUTION OF THE EUGLENID PELLICLE

BRIAN S. LEANDER,[1,2] RAFAL P. WITEK, AND MARK A. FARMER
Center for Ultrastructural Research, The University of Georgia, Athens, Georgia 30602
[1]*E-mail: bleander@interchange.ubc.edu*

Abstract.—Trends in the evolution of the euglenid pellicle were described using phylogenetic methods on 18S rDNA, morphological, and combined data from 25 mostly phototrophic taxa. The tree topology from a total-evidence analysis formed a template for a synthetic tree that took into account conflicting results derived from the partitioned datasets. Pellicle character states that can only be observed with the assistance of transmission and scanning electron microscopy were phylogenetically mapped onto the synthetic tree to test a set of previously established homology statements (inferences made independently from a cladogram). The results permitted us to more confidently infer the ancestral-derived polarities of character state transformations and provided a framework for understanding the key cytoskeletal innovations associated with the evolution of phototrophic euglenids. We specifically addressed the character evolution of (1) the maximum number of pellicle strips around the cell periphery; (2) the patterns of terminating strips near the cell posterior end; (3) the substructural morphology of pellicle strips; (4) the morphology of the cell posterior tip; and (5) patterns of pellicle pores on the cell surface.

Key words.—Character evolution, comparative morphology, 18S rDNA, electron microscopy, Euglenida, Euglenozoa, phylogeny.

Received February 16, 2001. Accepted August 16, 2001.

Euglenids are a distinct group of predominantly free-living unicellular flagellates that, according to 18S rDNA trees, diverged early in eukaryotic history (Sogin 1997; Gray et al. 1998). However, the position of euglenids within eukaryotes is uncertain—it can be significantly different in trees derived from a variety of protein genes (Keeling et al. 1998; Baldauf et al. 2000). The majority of euglenids are colorless heterotrophs, but the better-known taxa such as *Euglena gracilis* are green phototrophs that acquired their plastids a single time by way of a secondary symbiotic event involving a green algal prey cell (Gibbs 1978). The presence of plastids unites a large subclade of euglenids (Linton et al. 1999, 2000; Leander and Farmer 2001a; Leander et al. 2001).

Euglenids share a number of ultrastructural features (discoidal mitochondrial cristae, two or more flagella with paraxial rods), but the best synapomorphy for the group is a cortical cell region called the ''euglenid pellicle,'' which consists of the plasma membrane, proteinaceous strips arranged in parallel, subtending microtubules, and tubular cisternae of endoplasmic reticulum (Sommer 1965; Leander and Farmer 2001b). The most noticeable components of the pellicle are the strips, which articulate with adjacent strips along their lateral margins and may run longitudinally or helically around the anteroposterior axis of the cell (Fig. 1A, B). Longitudinally arranged strips are associated with cells that cannot alter their shape. In contrast, helical pellicles are often associated with a peculiar mode of cellular locomotion called ''euglenoid movement,'' which describes the wriggling or peristaltic-like movements that are caused when sliding occurs at the junctions between strips (Gallo and Shrével 1982; Suzaki and Williamson 1985, 1986a; Petersen-Mahrt 1997). The function of euglenoid movement is unknown, however, it evolved before the acquisition of chloroplasts within the group.

Studies of the pellicle not only provide important information about the phylogenetic relationships of euglenids (Leander and Farmer 2001a) but may also help us better understand the idiosyncratic nature of character evolution (Gould 1988, 1990, 1996). Once we are able to polarize character state series that are bordered by a relatively complex state on one end and a simpler state on the other, we may be able to document examples of reduction in morphological complexity. Within a robust phylogenetic context, we may also demonstrate intriguing examples of homoplasy that warrant cautious inferences about their adaptive or nonadaptive origin (Gould and Vrba 1982). This is particularly relevant to patterns of pellicle pores, comparisons of strip morphology, and patterns and numbers of strips (Leander and Farmer 2000a,b, 2001b).

Background on Pellicle Morphology

Pellicle pores

Pellicle pores are small openings in the pellicle positioned at the junctions between strips (articulation zones; Fig. 1C). The pores serve as openings to the cell surface for two distinct kinds of ejectile organelles: muciferous bodies and mucocysts (Hausmann 1978; Leander and Farmer 2000a). Most taxa possess muciferous bodies, which are saclike structures containing amorphous mucopolysaccharides (Hausmann and Mignot 1977; Fig. 1D, E). Some taxa, such as *Peranema* and *Entosiphon*, possess mucocysts, which are cylindrical structures composed of a latticelike framework of carbohydrate that maintains their elongated shape when rapidly discharged through a pore (Mignot and Hovasse 1973; Hilenski and Walne 1983; Fig. 1F). In most cases, pellicle pores are distributed over the cell surface without any obvious pattern. However, some taxa possess distinct patterns of pellicle pores where the number of strips between rows of pores is constant; three states have been recognized in different taxa: two, four, and eight strips (Leander and Farmer 2000a). Hypothetically, these states in different taxa were not the result of parallel evolution and are linked in this unpolarized order. The evo-

[2] Present address: Department of Botany, University of British Columbia, 3529-6270 University Boulevard, Vancouver, British Columbia V6T 1Z4, Canada.

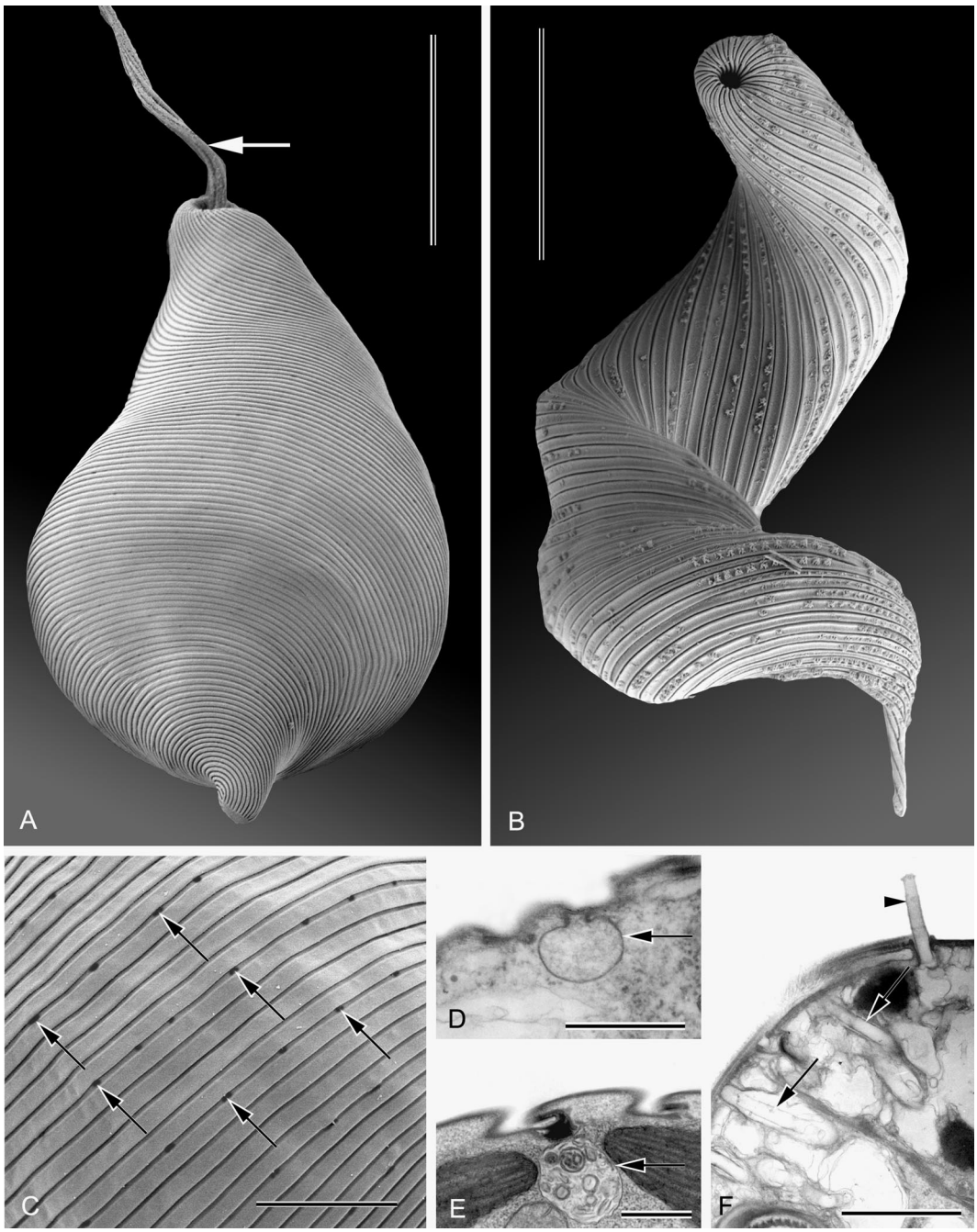

FIG. 1. Electron micrographs showing surface features of euglenid cells. (A) Scanning electron micrograph (SEM) of *Eutreptia pertyi* showing helically arranged pellicle strips and anteriorly directed flagella (arrow) emerging from the canal opening (bar = 10 μm). (B) SEM of *Euglena spirogyra* (without flagella) showing the contracted stage of its semirigid pellicle (bar = 10 μm). (C) SEM of *Euglena laciniata* showing four strips between rows of pellicle pores (arrows; bar = 5 μm). (D) Transmission electron micrograph (TEM) through a muciferous body (arrow) of *E. pertyi* (bar = 0.5 μm). (E) TEM through a muciferous body (arrow) of *E. laciniata* (bar = 0.5 μm). (F) TEM through nonfired mucocysts and an ejected mucocyst (arrowhead) of *Peranema trichophorum* (bar = 1 μm).

lution of these states, however, remains untested with molecular data and cladistic methods.

Strip morphology

Like patterns of pellicle pores, some characters associated with strip morphology have been suggested to consist of transformational series of character states (Suzaki and Williamson 1986b; Leander and Farmer 2001b). When viewed in transverse section each pellicle strip is usually S-shaped and composed of two major components: frames and strip projections (Fig. 2A–E). Frames form the fundamental S-shaped region of a strip (Leander and Farmer 2001b; Fig.

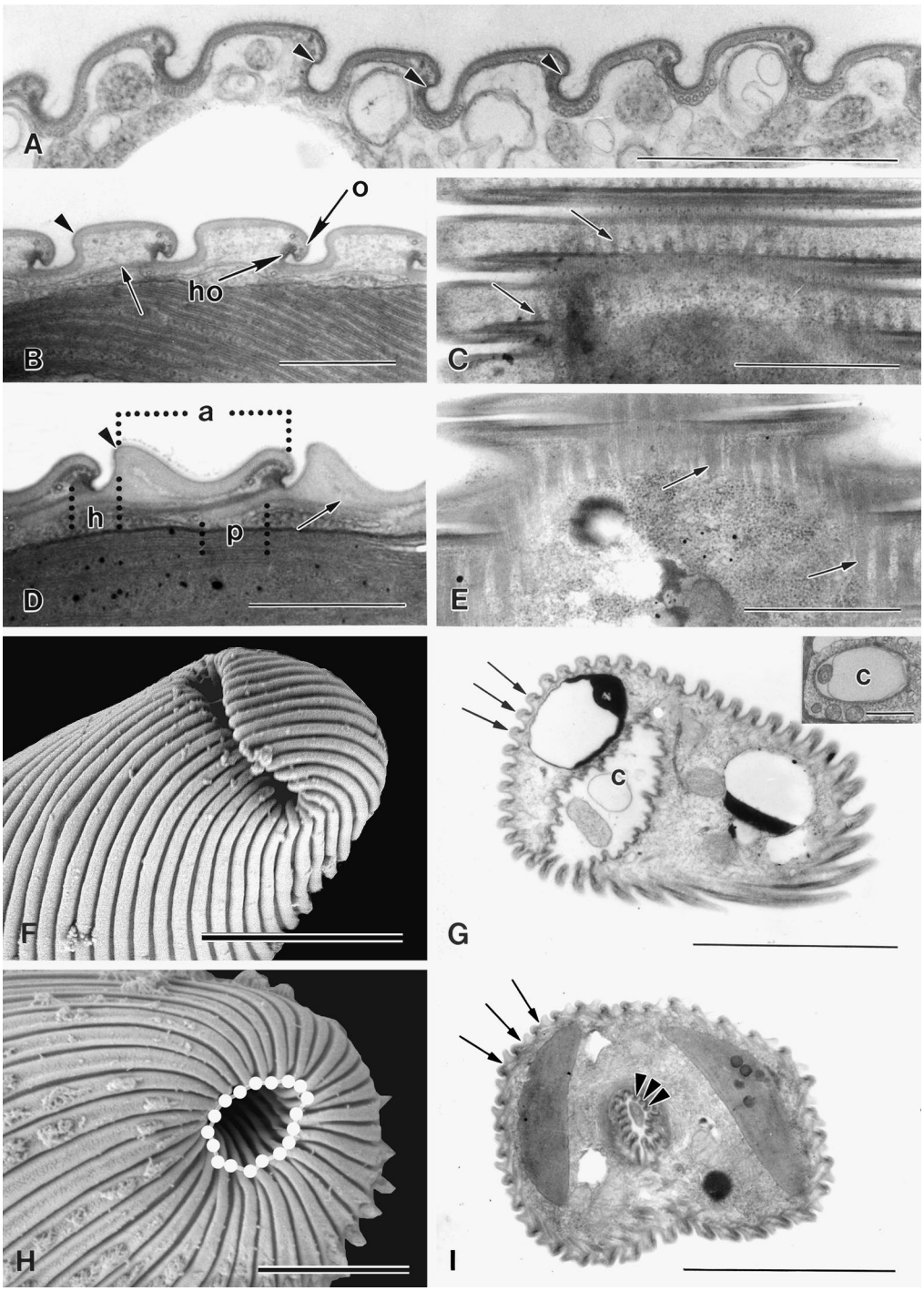

FIG. 2. (A–E) Transmission electron micrographs (TEM) showing substructural features of euglenid strips. (F–I) Electron micrographs showing patterns of terminating strip near the canal opening. (A) TEM through *Peranema trichophorum* showing the articulation zones (arrowheads) between plateau-shaped strips that lack distinct keels and strip projections (bar = 1 μm). (B) TEM through *Euglena laciniata* showing plateau-shaped strips with a distinct keel (arrowhead) and threadlike prearticular projections (arrow). The difference between the overhang (arrow, o) and the hook (arrow, ho) are also indicated (bar = 0.5 μm). (C) Tangential TEM through *E. laciniata* showing the prearticular projection in the form of linear threads (arrows), and the postarticular projections in the form of an indented plate (the pattern of fine vertical lines; bar = 1 μm). (D) TEM through *Euglena spirogyra* showing M-shaped strips with a distinct keel (arrowhead), postarticular projections (arrrow), and toothlike prearticular projections consisting of a basal plate (p). The difference between the arch (a) and the heel (h) are also indicated (bar = 0.5 μm). (E) Tangential TEM through *E. spirogyra* showing the prearticular projection in the form of robust teeth (arrows) and the postarticular projections in the form of an indented plate (the pattern of fine vertical lines; bar = 1 μm). (F) Scanning electron micrograph (SEM) of *Euglena mutabilis* showing a slitlike canal opening and the absence of terminating strips (bar = 2 μm). (G) TEM of *E. mutabilis* showing the maximum number of strips around the cell periphery (arrows), P. The canal (c) is lined by strips with weak structural integrity near the opening and is unlined near the reservoir (bar = 2 μm). Inset,

2B, D). In many taxa, strip projections branch laterally from the frames; those that are positioned below the frame of an adjacent strip are called ''prearticular projections'' and those positioned below the frame of the same strip are postarticular projections (Leander and Farmer 2001a,b; Fig. 2B–E). Many discrete character states that appear to be linked in evolutionary series have been recognized for frames and strip projections (Leander and Farmer 2001b). For example, prearticular projections can take the form of delicate strands, linear threads, robust teeth, and continuous plates. The first three states are periodic and differ in their thickness; toothlike prearticular projections also differ in that flattened projections stem from the upper surface of a basal plate (Leander and Farmer 2001b; Fig. 2D, E).

Surface patterns of strips

Comparative morphology of the pellicle indicates that euglenids may provide information about the evolution of development in unicellular eukaryotes. Euglenids are among the few protists that possess diverse morphological traits that appear to be controlled by a common developmental mechanism, the details of which are completely unknown at this time. The best example of such traits is associated with surface patterns of strips, which are a consequence of strips that terminate before reaching the anterior and posterior ends of the organism. In most phototrophic taxa, the number of strips around the cell periphery (P; Fig. 2G, I) is reduced exponentially as discrete whorls of terminating strips (Leander and Farmer 2000a,b, 2001a). Every alternate strip terminates on a whorl, and the strips in between continue either toward the posterior end or into an anterior invagination called the ''canal'' (Figs. 1B, 2F–I). At the posterior end, the continuing strips may terminate on a subsequent whorl or converge with other strips at the posterior tip (Fig. 3C–E). The number of whorls of strip reduction at the posterior end (W_P), the number of strips that converge at the posterior tip (T), and P are linked and can be related mathematically (Leander and Farmer 2000a). Most phototrophic taxa possess canals lined by strips (Fig. 2I) and a single whorl of strip reduction near the canal opening (Fig. 2H). In contrast, some taxa possess canals lined by strips but lack a distinct whorl of strip reduction near the canal opening (e.g., *P. trichophorum*, Nisbet 1974; *E. mutabilis*, Fig. 2F–G). It should be noted, however, that the strips just inside the canal opening of *E. mutabilis* do show hints of a whorl of strip reduction, where every other strip protrudes further into the canal lumen than the remaining strips (Fig. 2G).

Although exponential patterns of posterior strip reduction (e.g., $P \rightarrow P/2 \rightarrow P/4$) are the most common, linear and bilinear patterns have also been described in which a constant number of strips (i.e., slope = n) terminate on consecutive whorls (e.g., $P \rightarrow [P - n] \rightarrow [P - 2n]$ Leander and Farmer 2000a,b). The linear-based patterns are thought to be evolutionarily linked to exponential patterns and can be mathematically described by different equations (Leander and Farmer 2000a,b). Less organized patterns of strip reduction have also been observed (Fig. 3A, B), but how these states relate to whorled patterns is unclear. Addressing the evolution of P and W_P with molecular data will allow us to describe the prevalence of homoplasy in these characters and more confidently polarize their respective states. This should shed light on the underlying mechanism controlling the development of these patterns.

Background on Euglenid Phylogeny

Several papers have compared 18S rDNA sequences from various euglenid taxa (Montegut-Felkner and Triemer 1997; Linton et al. 1999, 2000; Preisfeld et al. 2000, 2001; Leander and Farmer 2001a; Müllner et al. 2001). Chloroplast genes such as *rbcL* and *16S rDNA* have been explored to some extent; however, they appear to provide significantly less phylogenetic signal than *18S rDNA* (Thompson et al. 1995; Milanowski et al. 2001). In general, the molecular studies have confirmed the following about euglenid phylogeny: (1) euglenids with helically arranged strips evolved from euglenids with longitudinally arranged strips; (2) the chloroplast originated monophyletically within euglenids possessing helical pellicles; (3) the chloroplast has been independently lost multiple times; (4) as presently defined most photosynthetic genera (e.g., *Euglena* and *Phacus*) are not monophyletic; and (5) cell rigidity evolved multiple times independently from an ancestor capable of euglenoid movement. Whether this emerging gene tree accurately reflects the organismal phylogeny of euglenids has yet to be thoroughly tested with morphological data. Moreover, to rebuild a classification system that accurately reflects genealogical relationships, it is desirable to identify unambiguous (morphological) synapomorphies that unite the newly recognized clades.

The present paper attempts to cladistically integrate a large morphological dataset from single-celled organisms into a molecular context. An earlier and more limited study compared 18S rDNA sequences and 62 morphological character states within 19 characters from 12 euglenid taxa (Leander and Farmer 2001a). We have expanded these datasets by providing new morphological data for 10 more euglenid taxa and five new 18S rDNA sequences. The broadened datasets permit us to outline the macroevolutionary history of euglenids more confidently and comprehensively, particularly with respect to P, W_P, strip projections, the morphology of the cell posterior tip, and surface patterns of pellicle pores. Pellicle character states were phylogenetically mapped onto a synthetic organismal tree inferred from analyses of partitioned data (pellicle morphology and 18S rDNA) and total evidence to test hypotheses regarding primary homology statements and character state polarities and determine which

←

TEM showing a transverse section through an unlined region of the canal (bar = 1 μm). (H) SEM of *E. spirogyra* showing an anterior whorl of strip reduction (*i*) near the canal opening. Each strip that terminates before entering the canal is marked by a white dot (bar = 2 μm). (I) TEM of *E. spirogyra* showing the maximum number of strips around the cell periphery (arrows), P, and the minimum number of strip lining the canal (arrowheads; bar = 3 μm).

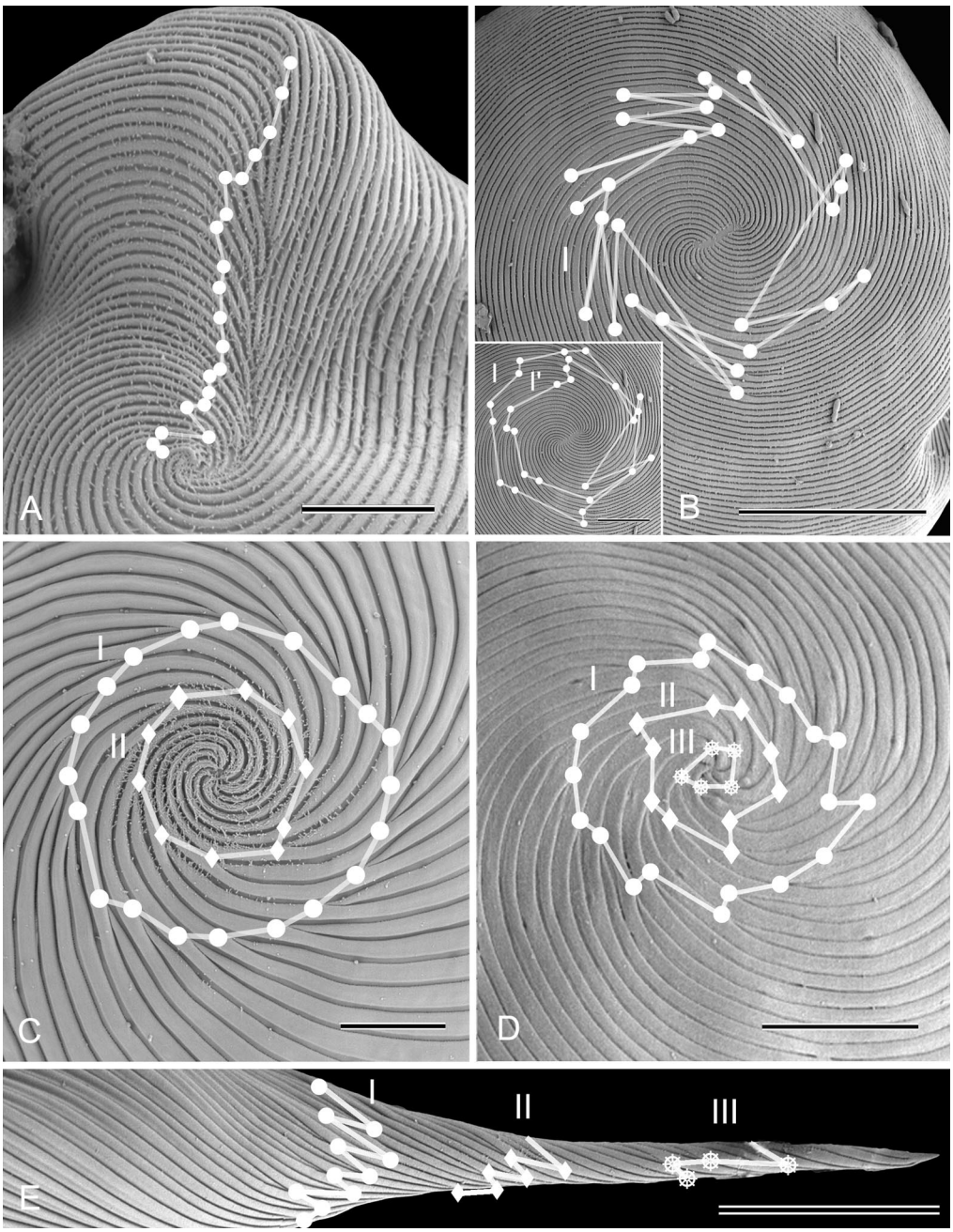

FIG. 3. Scanning electron micrographs (SEM) showing patterns of terminating strips at the posterior end of euglenids. (A) SEM of *Peranema trichophorum* showing an alternate pattern of terminating strips (dots) on one side of a common line of convergence (bar = 2.5 μm). (B) SEM of *Eutreptia pertyi* showing a single disorganized whorl of exponential strip reduction (bar = 10 μm). Inset, when every other terminating strip is connected by a line, two mostly nonoverlapping whorls emerge, where the outer whorl is denoted by I and the inner whorl by I′ (bar = 5 μm). (C) SEM of *Euglena laciniata* showing two whorls of exponential strip reduction (bar = 2.5 μm). (D) SEM of *Astasia longa* showing three whorls of exponential strip reduction on a rounded posterior end (bar = 2.5 μm). (E) SEM of *Euglena oxyuris* showing three whorls of exponential strip reduction on a sharply pointed posterior end (bar = 10 μm).

character states (if any) are the best candidates for apomorphy-based taxon definitions.

MATERIALS AND METHODS

Culture Conditions

The 25 taxa used in this study and their locations in culture collections are listed in Table 1. Morphological characters and culture requirements for 15 of these taxa have been reported previously (Leander and Farmer 2000a,b, 2001a,b). Characters relating to surface patterns of strips and pores for the remaining 10 taxa are reported here for the first time; these taxa are *Astasia longa*, *Colacium mucronatum*, *Euglena anabaena*, *E. cantabrica*, *E. laciniata*, *E. oxyuris*, *E. spirogyra*, *E. terricola*, *Eutreptia pertyi*, and *Peranema trichophorum*. *Astasia longa* was grown in a Polytomella medium (Starr

TABLE 1. Taxa examined in this study.

Taxon	Source[1]	Culture No.	GenBank
Astasia longa	UTEX	L 512	AF112871
Colacium mucronatum[2]	UTEX	LB 2524	AF326232
Distigma proteus	UTEX	LB 508	AF106036
Entosiphon sulcatum	wild: New Jersey	—	—
Euglena acus	UTEX	LB 1316	AF152104
Euglena anabaena	UTEX	373	AF242548
Euglena cantabrica[2]	UTEX	LB 1320	AF329972, AF329973
Euglena gracilis	UTEX	753	M12677
Euglena helicoideus	wild: Georgia	—	—
Euglena laciniata[2]	UTEX	LB 1312	AF326231
Euglena mutabilis	SAG	1224-9a	AF096992
Euglena myxocylindracea[2]	UTEX	1989	AF326233
Euglena oxyuris	wild: New Jersey[3]	—	AF090869
Euglena spirogyra	UTEX	LB 1307	AF150935
Euglena stellata	UTEX	372	AF150936
Euglena terricola[2]	UTEX	LB 1310	AF329974, AF329975
Euglena tripteris	UTEX	LB 1311	AF286210
Eutreptia pertyi	UTEX	LB 1290	AF081589
Lepocinclis buetschlii	UTEX	LB 523	AF096993
Lepocinclis ovata	UTEX	LB 1305	AF061338
Peranema trichophorum	CBSC	WW-13-1838	U84733, U84734
Petalomonas cantuscygni	CCAP	1259/1	U84731
Phacus brachykentron	UTEX	LB 1317	AF286209
Phacus oscillans[4]	UTEX	LB 1285	AF181968
Phacus pyrum	UTEX	LB 2345	AF112874

[1] ATCC, American Type Culture Collection; CBSC, Carolina Biological Supply Company, Burlington, NC; SAG, Sammlung von Algenkulturen Göttingen; UTEX, Culture Collection of Algae at the University of Texas, Austin, TX.
[2] Sequenced by the authors for this study.
[3] Provided by R. E. Triemer, Rutgers University, Piscataway, NJ.
[4] Labeled as ''*Phacus caudata*'' in the UTEX collection (see Linton et al. 2000).

and Zeikus 1993); *E. anabaena* was grown in a Proteose medium (Starr and Zeikus 1993); *E. cantabrica*, *E. laciniata*, and *E. terricola* were grown in a soil-water ($Gr+/NH_4$) medium (Starr and Zeikus 1993); *E. spirogyra* and *C. mucronatum* were grown in a soil-water medium enriched with a pea; *E. pertyi* was grown in a soil-seawater medium (Starr and Zeikus 1993); and *P. trichophorum* was grown in a *Peranema* medium (PER; The Culture Collection of Algae and Protozoa, Ambleside, Cumbria U.K.) containing Complan (H. J. Heinz Co., Ltd., Hayes Park, Middlesex, U.K.). *Euglena oxyuris* was prepared from wild samples. All cultures were grown at 20°C and 12/12 light/dark cycle.

Transmission Electron Microscopy

Cells were collected into 1.5-ml Eppendorf tubes and fixed in 2% glutaraldehyde in 0.1 M cacodylate buffer (pH = 7.2) at 4°C for 1 h. After two 15-min washes in 0.1 M cacodylate buffer, cells were postfixed in 1% O_SO_4 and buffer at 4°C for 1 h. The cells were washed with distilled water, dehydrated through a graded series of ethyl alcohols, and covered in acetone for two changes of 20 min. Acetone-resin mixtures were used to infiltrate the cells before being embedded in pure resin (Electron Microscopy Sciences, Fort Washington, PA). After the cells were centrifuged at high speed into the tip of an embedding capsule, the samples were polymerized at 60°C. Blocks were sectioned on a RMC MT-X ultramicrotome, poststained with uranyl acetate and lead citrate, and viewed under a JEOL 100 CXII Transmission Electron Microscope.

Scanning Electron Microscopy

Approximately 10 ml of liquid medium containing cells was transferred to a small petri dish containing a piece of filter paper mounted on the inner surface of the lid and saturated with 4% O_SO_4. The cells were fixed by O_SO_4 vapors for 30 min before five drops of 4% O_SO_4 were added directly into the liquid medium and fixed for an additional 30 min. The cells were transferred onto 8-μm polycarbonate membrane filters (Corning Separations Div., Acton, MA), dehydrated with a graded series of ethyl alcohol, and critical point dried with CO_2. Filters were mounted on stubs and sputter coated for 60 sec (153 Å) with gold. The cells were viewed under a LEO 982 scanning electron microscope (SEM; LEO Electron Microscopy, Inc., Oberkochen, Germany). SEM data were presented on black backgrounds using Adobe Photoshop 5.0 (Adobe Systems, San Jose, CA).

Terminology and Replicate Observations

The terms used to describe strip surface patterns and substructural morphology are in accordance with Leander and Farmer (2000a, 2001b). Whenever possible, P and W_P were scored for a minimum of 30 different cells per taxon and the mode and range of variation were reported. Exceptions include observations of only eight cells from a wild sample of *E. oxyuris* and 10 cells were used to score P in *P. trichophorum*.

Phylogenetic Analysis of Pellicle Characters

Seventy-nine character states within 24 morphological characters were scored for 25 euglenid taxa (Tables 2, 3).

TABLE 2. Twenty-four morphological characters and 79 states associated with the pellicle of euglenids.

Character	Character states
1. Orientation of strips	0, longitudinal; 1, helical; 2, semilongitudinal; 3, longitudinal with a posterior twist
2. Strips lining the canal	0, no; 1, yes
3. P[1]	0, 8–12; 1, 16; 2, 18–20; 3, 28–32; 4, 36–40; 5, 48–56; 6, 80
4. W_i[2]	0, 0; 1, 1
5. Posterior strip reduction	0, no; 1, yes
6. Pattern of posterior strip reduction	0, partial[3]; 1, linear/pseudolinear; 2, exponential/pseudoexponential; 3, bilinear
7. W_P[4]	0, 1; 1, 2; 2, 3
8. Pellicle pores	0, absent; 1, present
9. Strip number between pores[1]	0, 2; 1, 4; 2, 8
10. Ejectile organelle	0, mucocyst; 1, muciferous body
11. Pellicle plasticity	0, rigid; 1, semiplastic; 2, plastic
12. Transverse shape of cell	0, ovoid; 1, circular; 2, deltoid
13. Morphology of posterior end[5]	0, keeled; 1, rounded; 2, oblique; 3, conical; 4, sharp; 5, stubby
14. Overhang	0, no; 1, yes
15. Struts on arches	0, no; 1, yes
16. Shape of frames[6]	0, U-shaped; 1, S-shaped; 2, plateau; 3, M-shaped; 4, robust[7]
17. Minor grooves	0, no; 1, yes
18. Keel	0, no; 1, yes
19. Widths of arch and heel	0, heel $>$ 3 $\times$ arch; 1, arch $\approx$ heel; 2, arch $\approx$ 2 $\times$ heel; 3, arch $>$ 4 $\times$ heel; 4, arch $>$ 10 $\times$ heel
20. Prearticular projects	0, absent; 1, delicate; 2, threadlike; 3, toothlike; 4, dove-tailed; 5, platelike
21. Postarticular projections	0, absent; 1, threadlike; 2, indented plate; 3, toothlike; 4, platelike
22. Doublet identity	0, none; 1, heels; 2, articulation zones
23. Ribs on prearticular projections	0, no; 1, yes
24. Longitudinal furrow near canal	0, no; 1, yes

[1] Mode from 30 cells scored.
[2] W_i denotes the first anterior whorl of exponential strip reduction.
[3] Strips at the posterior end converge on a common line; most of the strips (41 of 50) terminate on one side of the line and show an alternate pattern of strip reduction.
[4] Excluding primed Roman numerals.
[5] Scored from relaxed cells.
[6] Cross-sections of strips positioned near the cell equator (i.e., not near the anterior or posterior ends).
[7] Thick frames with a median depression in the arch.

TABLE 3. Matrix of 24 morphological characters for 25 taxa used in the parsimony analysis to infer phylogenetic relationships. Character styles are: U, unordered character states; R, ordered character states. The symbols for the characters and character states are defined in Table 3. N, unknown; dashes, inapplicable characters.

	Character																							
Character style	R	U	U	U	U	U	R	U	R	U	R	U	U	U	U	U	U	U	U	U	U	U	U	U
Taxon	1	2	3	4	5	6	7	8	9	10	11	12	13	14	15	16	17	18	19	20	21	22	23	24
Petalomonas cantuscygni	0	0	0	0	0	—	—	0	—	N	0	0	0	0	0	0	0	0	0	0	0	0	0	0
Entosiphon sulcatum	0	0	0	0	0	—	—	0	—	0	0	0	1	0	0	1	0	0	1	0	0	1	0	0
Distigma proteus	1	0	2	0	0	—	—	0	—	1	2	1	1	1	0	1	0	0	2	0	0	0	0	0
Peranema trichophorum	1	1	5	0	1	0	—	1	—	0	2	1	2	1	0	2	0	0	2	0	0	0	0	0
Eutreptia pertyi	1	N	5	N	1	1	0	1	—	1	2	1	3	1	0	2	0	1	2	0	0	0	0	0
Euglena anabaena	1	1	4	1	1	2	1	1	—	1	2	1	3	1	0	2	0	1	2	1	2	0	0	0
Euglena cantabrica	1	1	5	1	1	2	0	1	0	1	2	1	1	1	0	3	0	1	2	2	2	0	0	0
Euglena laciniata	1	1	4	1	1	2	1	1	1	1	2	1	3	1	0	2	0	1	2	2	2	0	0	0
Euglena mutabilis	1	1	4	0	1	1	1	1	—	1	2	1	3	1	0	1	0	1	1	1	2	0	0	0
Euglena myxocylindracea	1	1	4	1	1	2	1	1	2	1	2	1	3	1	0	1	0	1	1	2	2	0	0	0
Euglena gracilis	1	1	4	1	1	2	2	1	—	1	2	1	1	1	0	2	0	1	2	1	1	0	0	0
Astasia longa	1	1	4	1	1	2	2	1	—	1	2	1	1	1	0	2	0	1	2	1	1	0	0	0
Colacium mucronatum	1	1	4	1	1	2	1	1	—	1	2	1	3	1	0	2	0	1	2	1	2	0	0	0
Euglena terricola	1	1	4	1	1	2	1	1	1	1	2	1	3	1	0	2	0	1	2	2	2	0	0	0
Euglena stellata	1	1	4	1	1	2	1	1	1	1	2	1	3	1	0	2	0	1	2	2	2	0	0	0
Euglena tripteris	1	1	3	1	1	2	2	0	—	1	1	2	4	1	1	4	0	1	3	3	2	0	0	0
Euglena helicoideus	1	1	6	1	1	3	2	0	—	1	1	0	4	1	0	4	1	1	3	5	4	0	1	1
Euglena oxyuris	1	1	5	1	1	2	2	0	—	1	1	0	4	1	0	4	1	1	3	5	4	0	1	1
Euglena spirogyra	1	1	4	1	1	2	2	0	—	1	1	0	4	1	0	4	0	1	3	3	2	0	0	0
Lepocinclis ovata	1	1	1	0	1	2	1	0	—	1	0	1	4	1	0	3	0	1	4	4	0	2	0	0
Phacus pyrum	1	1	1	0	1	2	1	0	—	1	0	1	4	1	0	3	0	1	4	4	0	2	0	0
Euglena acus	2	1	3	1	1	2	1	0	—	1	1	1	4	1	0	4	0	1	3	3	2	0	0	0
Lepocinclis buetschlii	2	1	3	1	1	2	1	0	—	1	1	1	5	1	0	4	0	1	3	3	2	0	0	0
Phacus brachykentron	3	1	3	1	1	2	1	0	—	1	0	0	5	1	0	4	0	1	3	3	3	0	0	0
Phacus oscillans	3	1	2	1	1	2	0	0	—	1	0	0	5	1	0	4	0	1	3	3	2	0	0	0

We included all available taxa that best reflected the amount of morphological diversity known to occur in phototrophic euglenids. The matrix of character states was heuristically analyzed using parsimony with PAUP* 4.0 (Swofford 1999). Four of the characters consisted of obvious intermediate states and were ordered: character 1, semilongitudinally arranged strips were assumed to bridge helically arranged strips and longitudinally arranged strips that become helically arranged at the posterior tip; character 7, $W_P = 2$ was assumed to bridge $W_P = 1$ and $W_P = 3$; character 9, number of strips between rows of pores = 4 was assumed to bridge the alternative states 2 and 8; character 11, a semiplastic pellicle was assumed to bridge plastic and rigid pellicles (Tables 2, 3). *Petalomonas cantuscygni* and *Entosiphon sulcatum* were chosen as outgroups because previous comparisons of 18S rDNA and morphology using kinetoplastids as the outgroup demonstrate that these taxa diverge before all other euglenids (Montegut-Felkner and Triemer 1997; Linton et al. 1999; Preisfeld et al. 2000; Leander et al. 2001). The support of each node on the most parsimonious tree(s) was estimated with decay indices using AutoDecay 4.0.2 (Eriksson 1998) and nonparametric bootstrap percentages (Felsenstein 1985) from 1000 replicates using PAUP* 4.0. The tree length, number of informative characters, retention index (RI), and consistency index (CI) were reported. MacClade 3.03 (Sinauer Associates, Sunderland, MA) was used to phylogenetically map character state changes.

DNA Isolation, Amplification, and Sequencing

Genomic DNA was extracted from *C. mucronatum*, *E. cantabrica*, *E. laciniata*, *E. myxocylindracea*, and *E. terricola* using a Chelex 100 resin (Bio-Rad, 143–2832, Hercules, CA) protocol described by Goff and Moon (1993). Sequences of 18S rDNA were amplified using polymerase-chain-reaction primers and a thermocycling protocol established previously for the group (Elwood et al. 1985; Montegut-Felkner and Triemer 1997; Preisfeld et al. 2000). The following primer pairs were used to amplify the genes in three fragments: 1AF, 5′-AAC CTG GTT GAT CCT GCC AGT-3′ and 516R, 5′-ACC AGA CTT GCC CTC C-3′; 300F, 5′-AGG GTT CGA TTC CGG AG-3′ and 1055R, 5′-CGG CCA TGC ACC ACC-3′; 1055F, 5′-GGT GGT GCA TGG CCG-3′ and 1520B, 5′-TGA TCC TTC TGC AGG TTC ACC TAC-3′; 300F and 1377R, 5′-ATC ATC TTT GCT CCC C-3′; 1377F, 5′-GGG GAG CAA AGA TGA T-3′ and 1520B. The amplified DNA fragments were sequenced in both directions using the same primers and a Perkin-Elmer (Norwalk, CT) 310 Genetic Analyzer following manufacture's protocols. Gene Runner 3.05 (Hastings Software, Inc., Hastings, NY) was used to align complimentary sequences and cross-validate the nucleotides in the 5′–3′ sequence. Visual examination of ABI chromatographs permitted us to resolve some ambiguities in the sequences.

Alignment and Phylogenetic Analysis of 18S rDNA

GenBank accession tags for the 18S rDNA sequences compared in this study are listed in Table 1. A manual alignment of the sequences was assisted using Sequence Alignment Editor (Se-Al 1.0; Rambaut 1996) and the 18S rDNA secondary structure of *E. gracilis*, *P. trichophorum*, and *P. cantuscygni* (Van de Peer et al. 1999; Linton et al. 2000); the final alignment is available on request. A total of 1653 base positions were unambiguously aligned and analyzed by parsimony and maximum-likelihood algorithms using *P. cantuscygni* and *D. proteus* as outgroups. In the parsimony analysis, nucleotides and gaps were treated as independent, unordered, character states of equal weight. A heuristic search was run using PAUP* 4.0 with ACCTRAN character state optimization, tree bisection reconnection (TBR) branch swapping, random stepwise addition of taxa, and MULTREES on. Decay indices (AutoDecay 4.0.2, Eriksson 1998) and nonparametric bootstrap values (Felsenstein 1985) from 1000 replicates were generated to evaluate the robustness of each node on the most parsimonious tree. The tree length, number of informative characters, CI, and RI were reported.

The maximum-likelihood analyses were performed using PAUP* 4.0 with empirical nucleotide frequencies and two substitution types corresponding to the Hasegawa-Kishino-Yano (HKY) model for nuclear encoded genes. A molecular clock was not enforced, TBR branch swapping was used, and starting branch lengths were obtained using the Rogers-Swofford approximation method. Ten replications with random addition of taxa were performed for each of 100 bootstrap replicates.

Total Evidence and Consensus

There is currently debate about how to deal with multiple datasets in phylogenetic analyses. Some systematists advocate on mainly philosophical grounds that all available data should be combined and analyzed by parsimony (Kluge 1989, 1998; Kluge and Wolf 1993; Chippindale and Wiens 1994). Alternatively, it has been argued on empirical grounds that independent datasets should never be combined but analyzed separately by data-appropriate methods (e.g., maximum likelihood for DNA sequences) and subsequently checked for topological congruence (Lanyon 1993; Miyamoto and Fitch 1995). The advantages and disadvantages for each approach have been reviewed elsewhere (Bull et al. 1993; de Queiroz 1993; Miyamoto and Fitch 1995; Huelsenbeck et al. 1996). We have followed a synthetic approach using criteria that was best described by Wiens (1998): (1) partition datasets that may have different phylogenetic histories (e.g., pellicle morphology and 18S rDNA); (2) run separate analyses on these datasets and evaluate the robustness of the resulting clades; and (3) perform a parsimony analysis on an unweighted character matrix of the combined data and judge the resulting tree(s) as the best hypothetical phylogeny, but consider questionable (collapse) any branches that conflict with well-supported branches from the separate analyses. In general, we also collapsed conflicting branches that were weakly supported in different analyses.

RESULTS

Pellicle Morphology of Newly Examined Euglenids

Surface patterns of pores and strips

Ultrastructural data were gathered from the 10 taxa listed in Table 4. All of these taxa possessed conspicuous pellicle

TABLE 4. Numbers of strips exponentially reduced on the pellicles of newly examined euglenids. P refers to the number of strips around the periphery; the range of variation is shown parenthetically below the mode. The frequency of the mode for P over the number of cells observed is positioned directly below each taxon. For each pair of numbers associated with the anterior and posterior whorls, the first refers to the number of strips entering a particular whorl and the second is the number of strips that continue through the whorl. Anterior and posterior whorls are labeled with lowercase and uppercase Roman numerals, respectively. N denotes an unknown state.

	Taxon							
Character	*Peranema trichophorum*[1] (6/10)	*Eutreptia pertyi* (15/30)	*Euglena anabaena* (25/30)	*Euglena cantabrica* (23/30)	*Euglena laciniata* (30/30)	*Euglena oxyuris*[2] (6/8)	*Euglena spirogyra*[3] (27/30)	*Euglena terricola* (18/30)
P	50 (50–56)	48 (44–54)	40 (32–50)	48 (46–56)	40 —	48 (46–48)	36 (28–36)	40 (32–42)
Anterior strip reduction								
i	—	N	40–20	48–24	40–20	48–24	36–18	40–20
Posterior strip reduction								
Partial[4]	50–29	—	—	—	—	—	—	—
I	—	48–24[5]	40–20	48–24	40–20	48–24	36–18	40–20
II	—	—	20–10	—	20–10	24–12	18–9	20–10
III	—	—	—	—	—	12–6	9–4[6]	—

[1] Strips at the posterior end converge on a common line; most of the strips terminate on one side of the line and show an alternate pattern of strip reduction (Fig. 3A).
[2] Scored from cells collected from the wild.
[3] Pseudoexponential pattern of strip reduction at posterior end.
[4] Does not form a whorled pattern of strip reduction (see footnote 1).
[5] Whorl(s) of terminating strips are scored as pseudolinear (Fig. 3B, inset).
[6] The whorl in which the exponential pattern breaks down.

pores but only *E. cantabrica*, *E. laciniata*, and *E. terricola* possessed distinct patterns in the distribution of the pores. The patterns of pores on *E. cantabrica* and *E. terricola* have been reported previously (Leander and Farmer 2000a); *E. laciniata* was like *E. terricola* and *E. stellata* (Leander and Farmer 2001a) in possessing four strips between rows of pellicle pores (Fig. 1C).

With regard to surface patterns of strips, *E. anabaena*, *E. laciniata*, *E. terricola*, and *C. mucronatum* had identical pellicles: $W_A = 1$, $W_P = 2$, and $P = 40$ (Fig. 3C, Table 4). The pellicles of *E. oxyuris* and *E. spirogyra* were similar in possessing a pointed posterior tip with $W_P = 3$ (Fig. 3E); however, the mode for $P = 48$ and 36, respectively (Table 4). Additionally, whorls I and II of *E. oxyuris* displayed a zigzag effect, where every other terminating strip was shifted in position along the anteroposterior axis of the cell relative to the remaining terminating strips on the respective whorl. The pellicle of *A. longa* was identical to *E. gracilis* (Leander and Farmer 2000a), where $W_P = 3$, $W_A = 1$, and $P = 40$. *Euglena cantabrica* possessed a rounded posterior end with $W_P = W_A = 1$ and $P = 48$ (Table 4).

The patterns of terminating strips at the posterior ends of *E. pertyi* and *P. trichophorum* were not consistent with the usual pattern of exponential strip reduction across distinct whorls. Half of the strips on the pellicle of *E. pertyi* ($P/2 = 24$) terminated before reaching the posterior tip (quantitatively, $W_P = 1$) in a cryptically organized fashion that may be described as pseudolinear (Fig. 3B, inset). When consecutive terminating strips were connected with straight lines, the result was a disordered configuration of zigzags (Fig. 3B). In contrast, when every other terminating strip was connected with a straight line, two mostly nonoverlapping whorls emerged (qualitatively, $W_P = 2$), where the outer whorl (whorl I) yielded three strips between consecutively terminating strips and the inner whorl (whorl I′) yielded two strips between consecutively terminating strips (Fig. 3B, inset). Like the linear pattern of strip reduction on *E. mutabilis* (Leander and Farmer 2000a), the same number of strips terminated on whorls I and I′ in *E. pertyi* (in this case 12). However, in all of 15 cells analyzed, whorl I showed incomplete separation from whorl I′ (Fig. 3B, inset), hence the descriptor ''pseudolinear.'' The remaining strips converged on a short linear region rather than a common point, as has been observed in most phototrophic taxa (Fig. 3B–D).

The pattern of terminating strips at the posterior end of *P. trichophorum* was novel in three respects: (1) like *E. pertyi*, the strips converged on a common line rather than a common point; (2) a majority of the strips (41 of 50) terminated on one side of this line and only these strips showed a pattern of alternately terminating strips; and (3) when terminating strips were connected by straight lines, the emerging pattern did not in any way resemble a whorl (i.e., was not circular; Fig. 3A). Because a pattern of alternately terminating strips was present without being associated with a complete halving event (exponential reduction), the pattern of strips at the posterior end of *P. trichophorum* may be described as partial reduction.

Strip substructure

Like *Distigma proteus*, the strips of *P. trichophorum* (Mignot 1965) and *E. pertyi* (Dawson and Walne 1991) were reported to lack strip projections. Appreciating the difficulty in demonstrating the absence of a character state, we have confirmed these observations (Fig. 2A). The frames of *P. trichophorum* and *E. pertyi* were similar overall, except that in *E. pertyi* a distinct keel was present, whereas in *P. trichophorum* the transition between the heel and the arch was more gradual (Fig. 2A). The strips of *E. anabaena* and *C. mucronatum* were similar to those of *E. gracilis* (Kirk and Juniper 1964; Schwelitz et al. 1970; Lefort-Tran et al. 1980; Dubreuil and Bouck 1985) and *A. longa* (Suzaki and Wil-

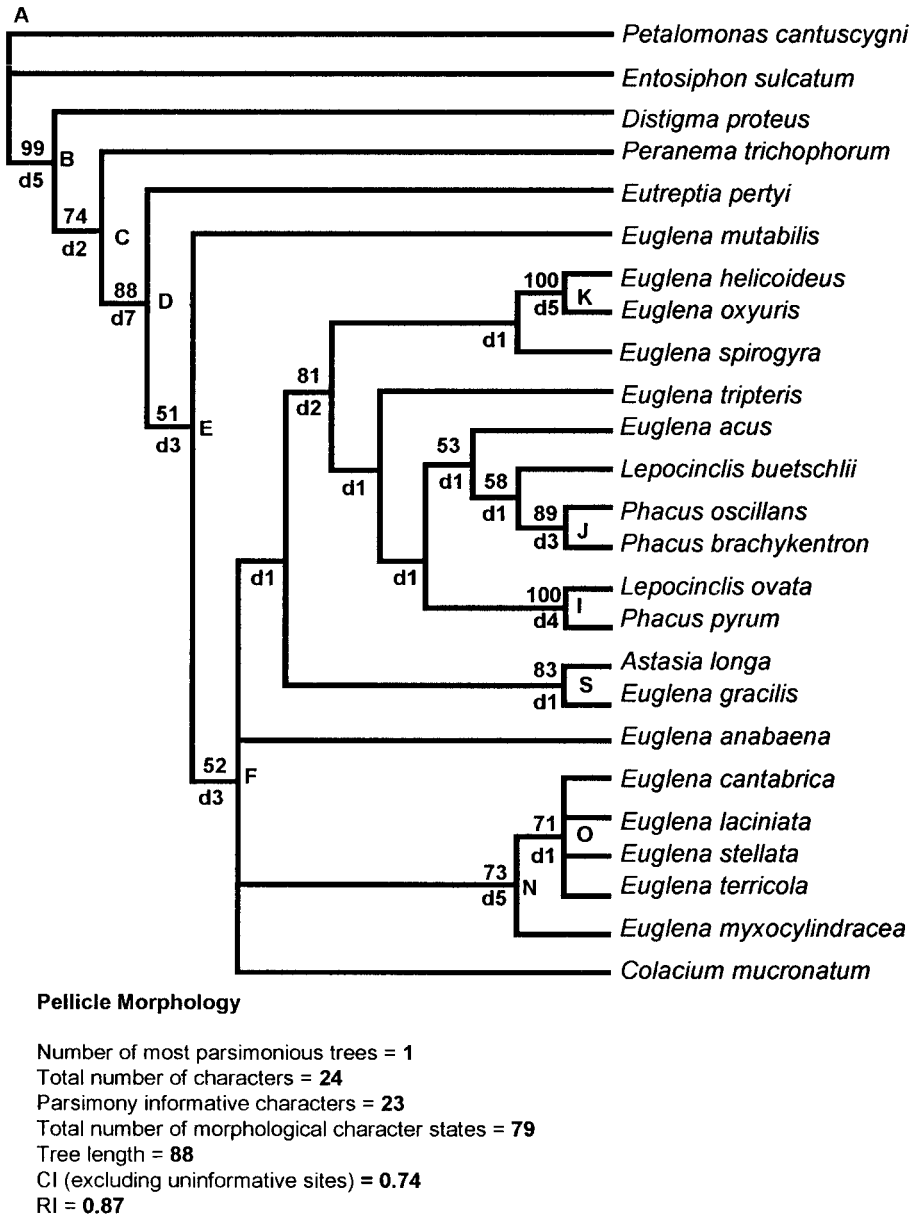

FIG. 4. The single most parsimonious tree derived from the data matrix of pellicle character states from 25 taxa (Table 3). The number above each stem are bootstrap percentages from 1000 replications; the symbols below each stem represent decay indices; letters at the nodes designate clades corresponding to Figure 6.

liamson 1986a); the frames were plateau-shaped, a distinct keel was present, and the prearticular projections formed delicate strands. The strips of *E. anabaena* and *C. mucronatum*, however, appeared to possess postarticular projections in the form of a delicate indented plate. The strips of *E. mutabilis* also possessed prearticular projections that formed delicate strands and postarticular projections in the form of a delicate indented plate; however, the frames were not plateau-shaped.

The frames of *E. laciniata* were plateau-shaped but with rather rounded arches (i.e., no evidence of a median depression). The strip projections were like those found in *E. terricola*, *E. cantabrica*, and *E. myxocylindracea* (Leander and Farmer 2001b): The prearticular projections formed linear threads and the postarticular projections formed a distinct indented plate (Fig. 2B, C). Leedale (1964) described the pellicle strips of *E. spirogyra* in some detail, but in reexamining the strips we concluded that the postarticular projections are in the form of an indented plate positioned directly above the toothlike prearticular projections (Fig. 2D, E).

Phylogenetic Analyses of Partitioned Data

Pellicle morphology

A parsimony analysis of the data presented in Tables 2 and 3 produced a single most parsimonious tree with a CI (excluding uninformative sites) = 0.74 and RI = 0.87 (Fig. 4). Five least inclusive clades (I, J, K, O, and S) were well

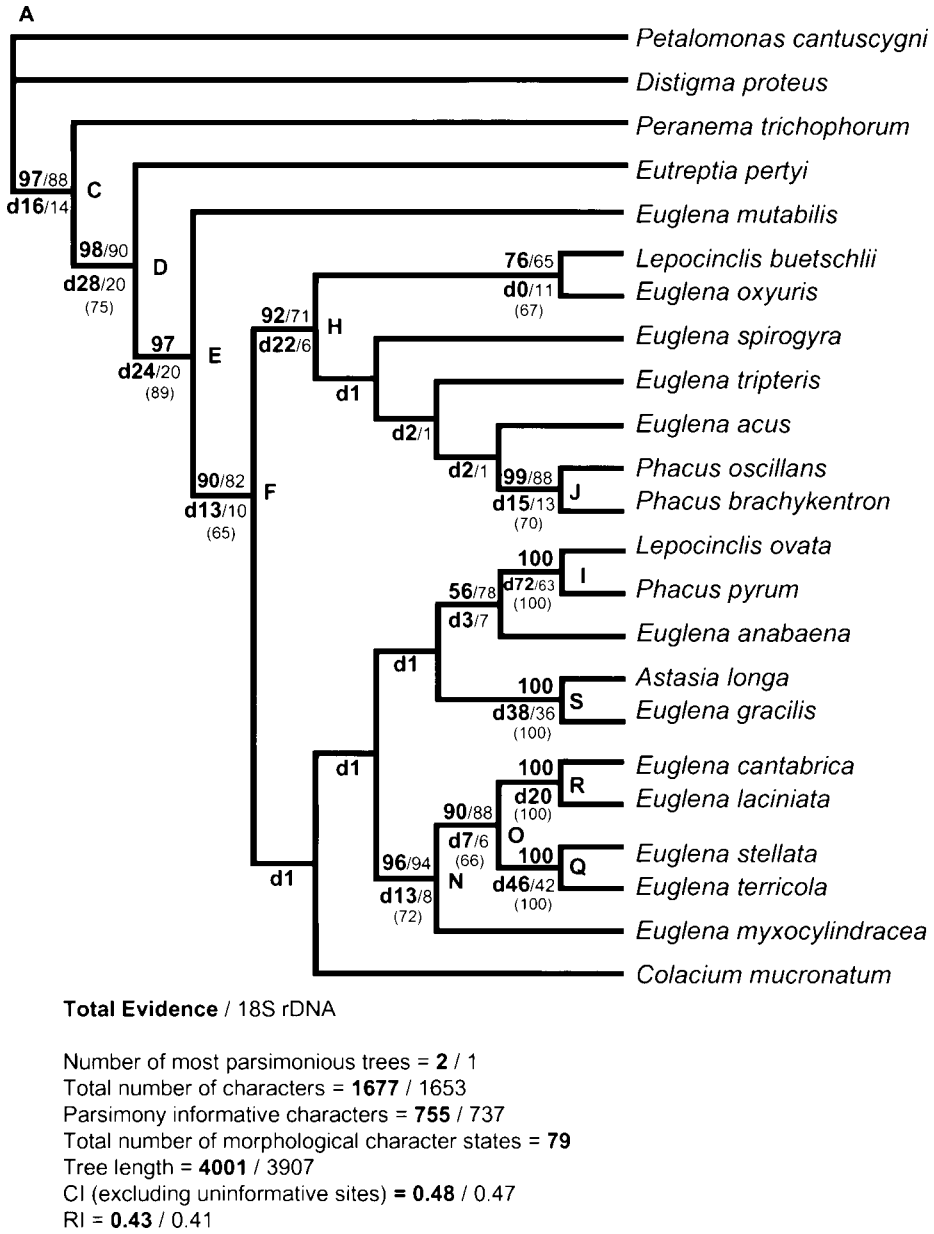

FIG. 5. One of the two most parsimonious trees derived from the combined dataset (i.e., total evidence), which matched the single most parsimonious tree derived from aligned 18S rDNA sequences from 23 euglenid taxa. Bootstrap percentages from 1000 replications and decay indices are shown above and below each stem, respectively. Values to the left were derived from the total evidence analysis and those to the right were derived from a separate analysis of the 18S rDNA sequences. The bootstrap percentages (from 100 replications) shown in parentheses were derived from a maximum-likelihood analysis on 18S rDNA sequences. Letters at the nodes designate clades corresponding to Figure 6.

supported by the data. *Euglena myxocylindracea* formed the sister taxon to clade O forming clade N. Clades I, J, K, and four other taxa clustered together to form a more inclusive group with good support (81% bootstrap; Fig. 4). The relationships among the taxa within this larger clade were weakly supported. The data showed *E. mutabilis* as the sister taxon to clade F forming the larger clade E. A nested sequence of increasingly more inclusive clades was formed by the addition of *E. pertyi*, *P. trichophorum*, and *D. proteus*, respectively (Fig. 4).

18S rDNA sequences

The tree generated from the maximum-likelihood algorithm produced four of the least inclusive clades (I, J, O, and S) present in the morphological tree. Because sequence data was unavailable for *E. helicoideus*, there was no way to independently examine clade K. Unlike the morphological tree, clade O contained two robust subclades: R and Q (Fig. 5). As in the morphological tree, *E. myxocylindracea* and clade O formed the more inclusive clade N, the taxa from *L. buetschlii* through *P. pyrum* clustered together, and both *E.*

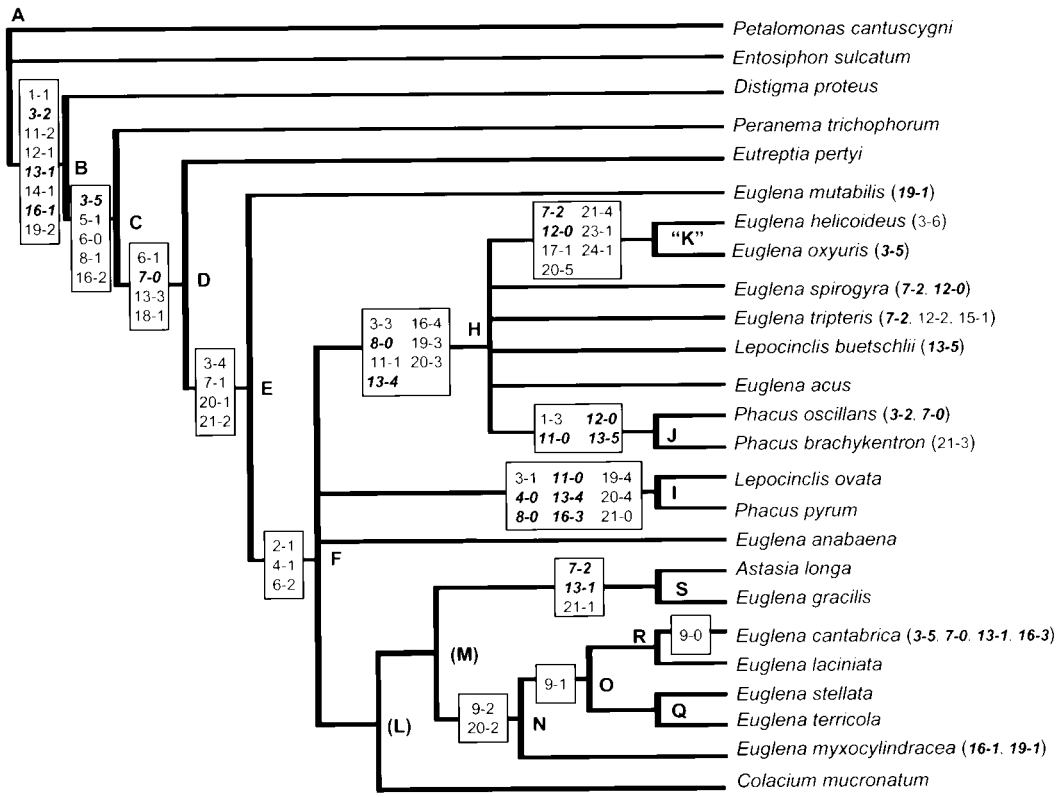

FIG. 6. A synthetic tree inferred from the topologies from both the combined and partitioned analyses. Most of the morphological character states associated with the euglenid pellicle have been parsimoniously mapped onto the tree. The two numbers separated by a dash represent each apomorphy; the first refers to the character and the second refers to the respective character state (Tables 2, 3). Autapomorphies are shown to the right of each taxon and homoplastic character states are shown in bold and italics. Bold letters refer to nodes strongly supported by both datasets. Letters in parentheses refer to nodes that were weakly supported but consistent with analyses of 18S rDNA. The quotes around clade K indicate that it is strongly supported by the morphological data (18S rDNA was not available for *Euglena helicoideus*).

mutabilis and *E. pertyi* maintained their same positions relative to the rest of the taxa. In contrast to the topology derived from the morphological data, the maximum-likelihood tree suggested: (1) *E. anabaena* was the sister taxon to clade I; (2) clade S clusters with clade N; and (3) *L. buetschlii* is the sister taxon to *E. oxyuris* (Figs. 4, 5).

Except for three notable differences, the parsimony analysis produced one tree with a topology that was quite similar to the maximum-likelihood tree (Fig. 5). The deepest point of discordance involved a group consisting of clade I and *E. anabaena*, where in the parsimony analysis it formed the sister group to clade S and in the maximum-likelihood analysis it formed the sister group to clade H. Except for clade J and the group consisting of *L. buetschlii* and *E. oxyuris*, the relationships of the taxa within clade H were not congruent between the two analyses. Like the morphological tree, there was strong support (88% bootstrap, decay index = 14) in the parsimony analysis of 18S rDNA showing *P. trichophorum* as the sister taxon to clade D (Figs. 4, 5).

Total Evidence

The combined dataset produced two most parsimonious trees, one of which exactly matched the topology resulting from the parsimony analysis of 18S rDNA sequences (Fig. 5). This is not surprising because there were many more parsimony informative characters from the 18S rDNA dataset (737 characters) than from the morphological dataset (23 characters). However, the total-evidence analysis was useful in boosting statistical support for nodes supported by both datasets and shrinking support for any nodes in conflict (Fig. 5). The total-evidence approach also maintained any nodes that were resolved by the analysis of 18S rDNA but could not be resolved by the analysis of morphological characters (e.g., clades Q and R; Figs. 4, 5). The second tree differed only in the position of *L. buetschlii*, where the *L. buetschlii–E. oxyuris* clade collapsed and *L. buetschlii* formed a sister taxon to a group consisting of *E. oxyuris* through *P. brachykentron*.

DISCUSSION

A Synthetic Tree

The total-evidence tree provided a template for a synthetic tree that best reflects the available data (Figs. 5, 6). Although topological differences did exist, none of the partitioned analyses produced nodes that strongly conflicted with the total-evidence tree. Nodes in the total-evidence tree that were both weakly supported and in conflict with one of the partitioned analyses (e.g., many nodes within clade H) were collapsed in the synthetic tree. The position of clade I was collapsed

within clade F because all three analyses gave conflicting results. Although morphologically dissimilar in many ways, *E. anabaena* clustered weakly with clade I in the analyses of 18S rDNA sequences, but this group did not occur in the morphological tree. Accordingly, *E. anabaena* was also collapsed within clade F (Fig. 6). Except for clades K and J, the interrelationships between the taxa within clade H were weakly supported in all analyses and remain ambiguous. Both the maximum-likelihood analysis of 18S rDNA and the analysis of pellicle characters suggest that *E. spirogyra* is a sister taxon to clade K; also, the parsimony analyses of the combined and partitioned datasets suggest that *E. acus* is a sister taxon to clade J. Because these relationships were only weakly supported and conflicted with the results of other analyses, they were left unresolved within clade H (Fig. 6).

The positions of *E. tripteris* and *L. buetschlii* within clade H were also problematic. For example, *L. buetschlii* clustered with *E. oxyuris* in the molecular and combined analyses and clustered with clade J in the separate analysis of pellicle morphology. This discrepancy may be the result of too few characters in the morphological analysis, and the molecular data may provide the more accurate picture. This suspicion is fueled by the fact that *L. buetschlii*, *E. oxyuris*, and *E. spirogyra* can be united by the presence of nonpellicle morphological features (e.g., link-shaped paramylon grains). Nonetheless, we have taken a conservative approach by leaving this putative relationship off of the synthetic tree and anticipate that analyses of new sources of data (e.g., 18S rDNA sequence for *E. helicoideus* and other morphological markers) will further clarify the issue.

In the separate analysis of pellicle morphology, clade S formed a weakly supported sister group to a clade consisting of the taxa within clades H and I (Figs. 4, 6). This relationship was caused by a single state change, $W_P = 3$ (7-2, Table 2), of a character that may be prone to homoplasy (Leander and Farmer 2001a). Clade S formed the sister group to clade N in both the combined and molecular analyses. Even though clade M is weakly supported in our analyses, we decided to retain this clade in the synthetic tree because members of clades S and N clustered together with strong support in previous studies of 18S rDNA (Linton et al. 1999, 2000). Moreover, we retained the position of *C. mucronatum* within clade L in the synthetic tree because it was present in all of the molecular analyses and was simply left unresolved within clade F in the morphological tree.

Once pellicle character states were mapped onto the synthetic tree, it became apparent that some nodes were supported by many state changes and others were supported by few or no state changes (Fig. 6). For instance, very few pellicle character states enabled us to tease apart the relationships between the taxa in clade L, which was weakly supported overall. Also, comparative morphology of the pellicle currently does not permit us to confidently infer the phylogenetic position of clade I. However, evidence from the pellicle does suggest that clade I is very well supported and is either sister to or belongs within clade H (Leander and Farmer 2001a; Fig. 4). The pellicle character states uniting various taxa within clade H were generally not supported by analyses of 18S rDNA. The nodes that were supported by a large

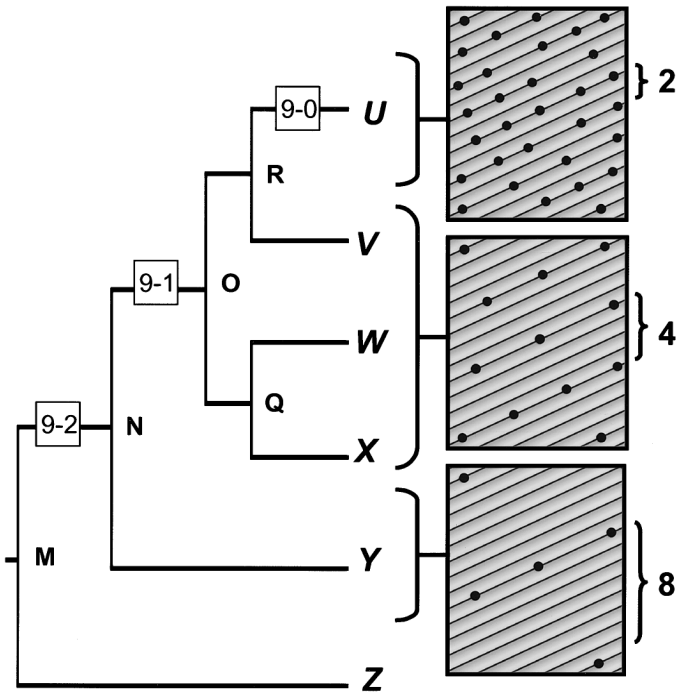

FIG. 7. Diagram illustrating the evolution of patterns of pellicle pore. Letters at the nodes correspond to Figure 6 and numbers separated by dashes denote the relevant character states (Tables 2, 3). The italicized letters *U–Z* refer to the respective taxa in clade M, where the outgroup *Z* = clade S (Fig. 6).

number of pellicle character states were also well supported by the molecular data (Figs. 5, 6).

In summary, the nodes on the synthetic tree with very strong support from both datasets were B, C, D, E, F, H, I, J, N, O, Q, R, and S (Fig. 5). Clade K was strongly supported by the morphological data and is currently not testable with molecular data. The nodes on the synthetic tree that were weakly supported but consistent with our molecular data and other phylogenetic analyses of molecular data were L and M (shown in parentheses in Fig. 6; Linton et al. 2000). With this data in hand, we were able to infer a great deal about the evolutionary histories of specific pellicle characters.

The Evolution of Pellicle Pores

The presence of pellicle pores over the cell surface of euglenids can range from being sparsely distributed to copious, and in some taxa, a constant number of strips resides between discrete rows of pores (Leander and Farmer 2000a; Fig. 1C). The ancestral state for clade C is the presence of pellicle pores that are distributed over the cell without any obvious pattern (state 8-1, Table 2); a state that has been retained in *P. trichophorum*, *E. pertyi*, *E. anabaena*, *C. mucronatum*, and clade S. Pores appear to have been lost altogether in clade H. An organized pattern of pores is a good synapomorphy for clade N (character 9, Table 2), where the states for the number of strips between rows of pores differ by a power of two. The cladistic analyses have permitted us to infer the polarity of these states (Fig. 7). A small number of pores with eight strips between pore rows is the ancestral state for clade N (state 9-2), where the density of pores grad-

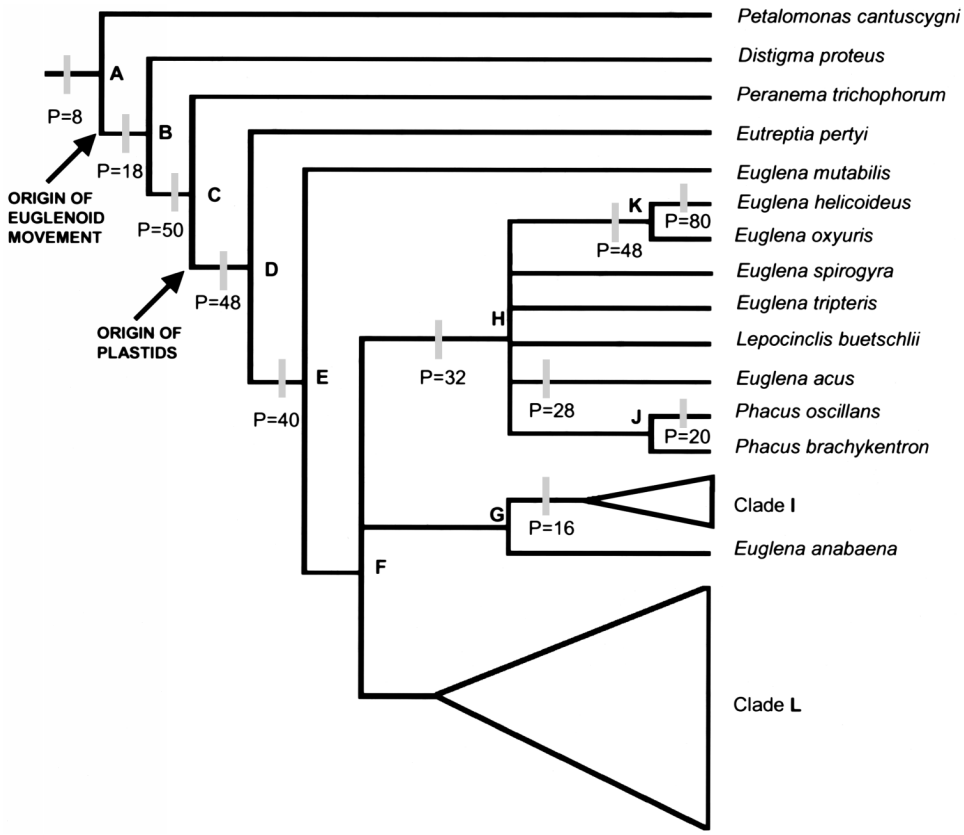

FIG. 8. An illustration of trends in the evolution of P, the maximum number of strips around the cell periphery. The states for P listed in Table 2 (character 3) have been parsimoniously mapped onto the synthetic tree (Fig. 6). See text for discussion.

ually increased within patterns with four and two strips between pore rows (Fig. 7). A related trend within clade N is that the number of strips between pore rows incurred two consecutive halving events ($8 \rightarrow 4 \rightarrow 2$). A higher density of pores provides the means for secreting mucus more quickly or more abundantly, which could be advantageous for any organism that must frequently form protective cysts in an environment prone to stochastic episodes of desiccation.

The Evolution of P

P refers to the maximum number of strips surrounding the periphery of the cell, where the value for P usually reflects a strong mode within a range of variation (Table 4; Leander and Farmer 2000a, 2001a). Colorless euglenids with longitidinal pellicles (e.g., *Petalomonas*, *Ploeotia*, and *Entosiphon*) possess between eight and 12 strips, and because these taxa diverge early in cladistic analyses (Leander et al. 2001), we infer that the ancestral euglenid possessed 10 or fewer strips (state 3-0, Table 2; Figs. 6, 8). The origin of helical pellicles appears to be associated with a permanent strip-doubling event in the common ancestor of clade B, where the value of P rose to 18–20 (state 3-2, Table 2; Leander and Farmer 2000a,b). Our results also indicate that a second strip-doubling event occurred prior to the common ancestor of clade C, where the value of P rose to 48–50 as in *P. trichophorum* and *E. pertyi* (state 3-5, Table 2; Figs. 6, 8). Strip-doubling events are consistent with our understanding of cell division in euglenids, where the value of P doubles just before cytokinesis and usually each daughter cell receives half of these strips (reestablishing the parental value of P) in a semiconservative manner (Mignot et al. 1987; Bouck and Ngo 1996). Thus, a permanent doubling event in any particular lineage is inferred to be a consequence of an ancestral cell that duplicated its cytoskeleton without ever undergoing cytokinesis (Leander and Farmer 2001a).

Taxa with few longitudinal strips (> 12) are rigid and limited to osmotrophic or bacteriotrophic modes of feeding. Taxa with at least 18 helically arranged strips are capable of euglenoid movement, and some of these can ingest very large prey such as other eukaryotes. The prey can actually be as large or larger than the euglenid predator, which is a mode of feeding that would necessitate a plastic pellicle (Triemer 1997). Euglenoid movement proceeds when adjacent strips slide relative to one another along their zones of articulation (the sliding strip model, Suzaki and Williamson 1985, 1986a; Fig. 2A, B). An increase in the number of strips equals both an increase in the number of articulation zones between strips and, consequently, a less constrained or rigid pellicle. Thus, fortuitous doublings in the number of strips may have provided the degree of cytoskeletal plasticity necessary for euglenoid movement and by consequence eukaryotrophic modes of feeding (Leander et al. 2001). By extension, a permanent increase in the number of strips ultimately led to the engulfment of chlorophyte prey and the secondary endosym-

biotic origin of euglenid plastids (Gibbs 1978). Our findings firmly support this scenario (Figs. 5, 8).

Once plastids became established within euglenid cells, P decreased in value (Fig. 8). Clade E is united by a reduction of P from about 48 (state 3-5, Table 2) to 40 (state 3-4, Table 2), where the latter value appears to be extremely stable within the phototrophs (Fig. 8). P then further decreased to 32 (state 3-3, Table 2) in the common ancestor of clade H, which is an inference supported by the following data: (1) more than three taxa within the clade possess P = 32 for every cell observed (i.e., no range of variation); (2) 32 is the median value in the range for P in *E. spirogyra*; and (3) the range in *E. acus* includes a proportion of cells with P = 32 (Leander and Farmer 2001a; Table 4; Figs. 6, 8). Within clade F, P decreased below 32 at least three times independently, namely in *E. acus* (P = 28), *P. oscillans* (P = 20), and clade I (P = 16; Fig. 8). The reductions in the latter two examples are associated with the convergent evolution of smaller cell size and cell rigidity. The reduction in strip number in clade I is inferred to be the result of a permanent halving event, where an ancestral cell underwent cytokinesis before the pellicular cytoskeleton was duplicated (Leander and Farmer 2001a). The independent decreases in P within clade F supports the hypothesis that once plastids were established euglenoid movement and eukaryotrophy were expendable.

P secondarily increased above the value of 40 at least two times independently, namely in *E. cantabrica* and clade K (Figs. 6, 8). Both of these increases are associated with a relatively large cell size. The value of P increased along the lineage leading to *E. helicoideus*, where P went from 32 to 48 to 80 (Figs. 6, 8). The transformation from P = 48 to 80 is inferred to represent a tertiary strip doubling event along this lineage (Leander and Farmer 2000b). In addition, the large cell sizes and large values for P in clade K are associated with the largest and thickest strips known in euglenids (Suzaki and Williamson 1986b; Leander and Farmer 2001b).

The Evolution of W_P

W_P refers to the number of whorls of terminating strips at the posterior end of euglenid cells. The ancestral state for euglenids is $W_P = 0$ (state 5-0, Table 2), a state found in taxa with both longitudinal and helical pellicles (Angeler et al. 1999; Leander and Farmer 2000a, 2001a; Leander et al. 2001). It was parsimoniously hypothesized that an exponential pattern with $W_P = 1$ evolved before $W_P = 2$ which evolved before $W_P = 3$ and that a linear pattern with $W_P = 3$ was derived from an exponential pattern with $W_P = 2$ (Leander and Farmer 2000a). Our comparative analyses indicate that this scenario is only partially correct. The pattern of terminating strips on the posterior end of *E. pertyi* suggests that a single strip halving event ($W_P = 1$ excluding primed whorls) did evolve prior to $W_P = 2$, but it did so in a pseudolinear fashion (Fig. 3B). Although P was halved at the posterior end, the pattern of terminating strips did not form a single distinct whorl; the pattern formed two mostly nonoverlapping whorls that closely resembled whorls I and I′ of *E. mutabilis* (Leander and Farmer 2000a). Mapping these states onto the topology of Figure 6 suggests that $W_P = 3$ within the linear pattern of *E. mutabilis* was not a derived state but instead evolved prior to $W_P = 2$ within an exponential pattern (Fig. 9). In this scenario, whorls I and I′ eventually coalesced into a single distinct whorl forming the exponential pattern with $W_P = 2$ (Figs. 3C, 9).

The states $W_P = 1$ and $W_P = 3$ evolved from the relatively common state of $W_P = 2$, and these character state transformations occurred multiple times independently (Fig. 9). $W_P = 3$ is present in clade S, clade K, and two unresolved taxa within clade H, namely *E. spirogyra* and *E. tripteris*. As originally hypothesized (Leander and Farmer 2000b), our analyses confirm that $W_P = 5$ within the bilinear pattern of *E. helicoideus* was derived from $W_P = 3$ within an exponential pattern (Fig. 9). This is supported not only by the cladistic analyses but by the zigzag effect on whorls I and II of *E. oxyuris* (Fig. 3E), which is interpreted to be a preliminary stage of one whorl separating into two homologous whorls.

A reduction from $W_P = 2$ to $W_P = 1$ has occurred at least twice (Fig. 9). In *P. oscillans*, the elimination of one whorl appears to be associated with a permanent strip reduction event, where P decreased from a value of 32 to 20 (Leander and Farmer 2001a; Figs. 8, 9). In contrast, the independent reduction of W_P in *E. cantabrica* is associated with a slight increase in the number of strips where the value of P jumped from 40 to 48. Also, the posterior end of *E. cantabrica* is markedly more broad and rounded compared to all of the other taxa in the analysis, but whether this has anything to do with the reduction in W_P is unclear.

The value for W_P and the associated pattern of strip reduction (e.g., exponential vs. linear) might be interpreted to be a consequence of optimal packing under the constraints produced by the number of strips (P), the thickness and spacing of the strips, the size of the cell, and the shape of the cell posterior tip. If this were the case, then any two taxa with the same characteristics listed above should possess the same value for W_P. However, *E. tripteris* and *E. acus* have more or less the same relevant pellicle features, but $W_P = 3$ and $W_P = 2$, respectively. Under the optimal packing hypothesis, if all else was about equal except for the shape of the posterior tip in two different taxa (blunt vs. sharp), then we might expect the value of W_P to differ. However, *L. buetschlii* (blunt posterior tip) and *E. acus* (sharp posterior tip) fit this scenario, but both taxa possess $W_P = 2$. Moreover, the taxa in clade S and clade Q (Fig. 5) have identical states relating to cell size, the number of strips, and the width and spacing of the strips for most of the cell length, but members of clade Q possess a pointier posterior tip. One might predict that given the packing constraints on a pointed posterior tip, W_P would be greater in clade Q. The opposite actually occurs, where clade S (with more rounded posterior tips) possesses $W_P = 3$ and clade Q possesses $W_P = 2$ (Fig. 3C, D). The strips in clade Q (Fig. 3C) achieve $W_P = 2$ by decreasing their width as they move toward the extreme posterior tip. Together, these data indicate that the morphogenesis of terminating strip patterns on the posterior end of euglenid cells is more complicated than the optimal packing hypothesis. Unfortunately, at this time, almost nothing is known about these processes.

We suspect that, in general, the states for W_P have little if anything to do with fitness; however, they do provide useful

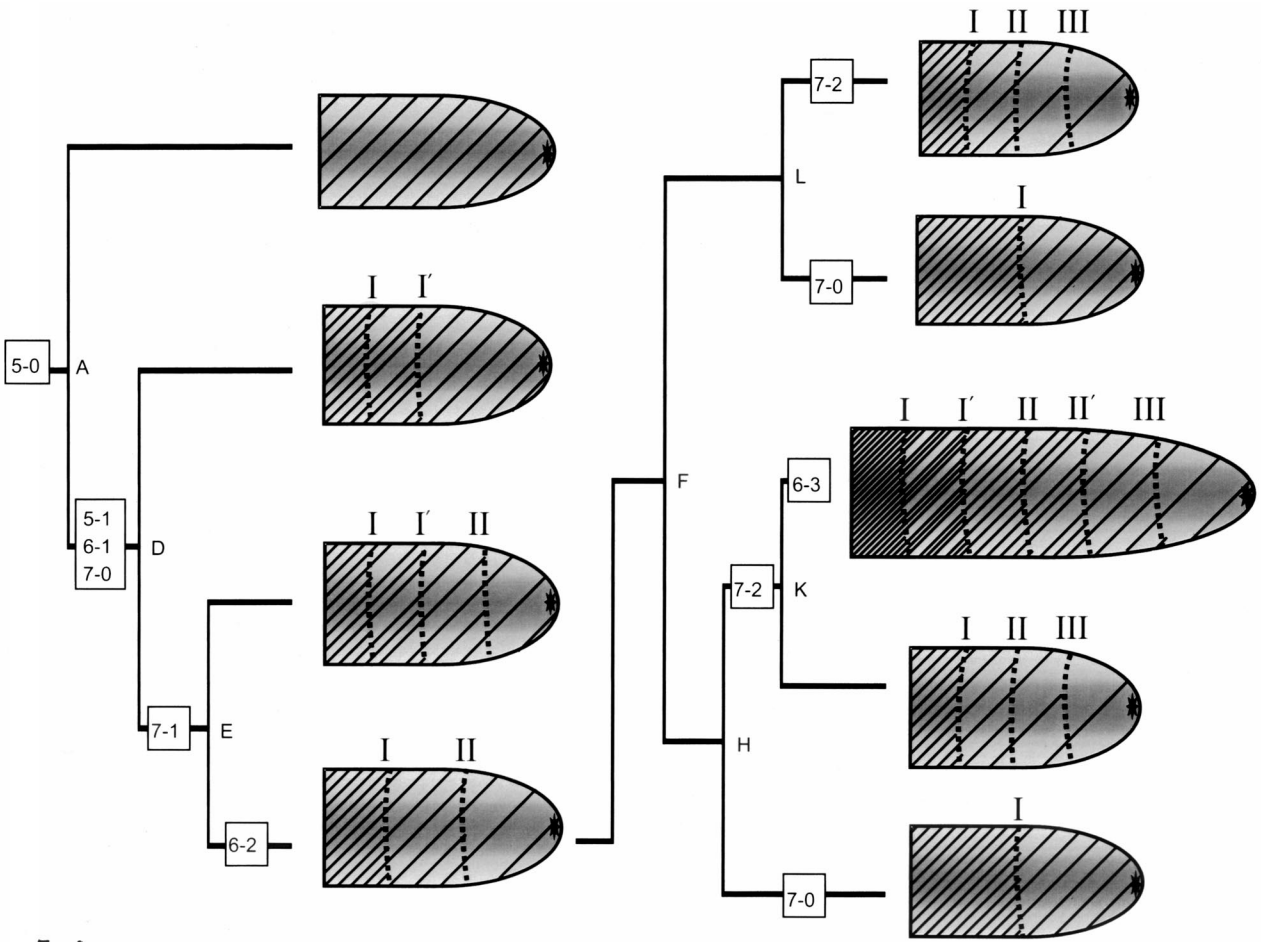

FIG. 9. Diagram illustrating the character evolution of W_P, the number of whorls of terminating strips near the posterior end of euglenid cells. Letters at the nodes correspond to Figure 6 and numbers separated by dashes denote the relevant character states (Tables 2, 3). Roman numerals mark each whorl of strip reduction as defined previously (Leander and Farmer 2000a), where primed numerals reflect the separation of one whorl into two homologous whorls. The results show that pseudolinear and linear patterns of strip reduction (state 6-1, Table 2) evolved before exponential patterns (state 6-2, Table 2). The bilinear pattern is derived from an exponential pattern with $W_P = 3$ (clade K). $W_P = 1$ and $W_P = 3$ each evolved at least two times independently from $W_P = 2$.

phylogenetic information. The best example is the morphological connection of *E. pertyi* with *E. mutabilis* (Fig. 9), where without this information the phylogenetic position of *E. mutabilis* in 18S rDNA trees would be difficult to interpret. The presence of distinct whorls of strip reduction has been found only in taxa that either possess plastids or have lost them secondarily. This information alone has paleontological value in that it is useful for interpreting whether a particular fossil is actually a euglenid and if so, whether it was phototrophic. For example, the acritarch *Moyeria* from Ordovician and Silurian sediments not only possesses striplike structures but also has what appear to be whorls of exponential strip reduction (Gray and Boucot 1989). Knowing this permits us to more confidently infer that plastids were present in euglenids at least 450 million years ago.

The Evolution of Frames

A fairly messy set of character state transformations is associated with the frames of strips. For example, M-shaped (including robust-type) frames (states 16-3 and 16-4, Table 2) evolved convergently at least twice: (1) the M-shaped frames of *E. cantabrica* evolved within clade N; and (2) robust M-shaped frames evolved in the common ancestor of clade H. The extremely broad frames in clade I are also M-shaped, but whether these frames are derived within clade H or are the result of a third case of convergent evolution is still unclear. If *E. anabaena*, which does not have M-shaped frames, is actually the sister taxon to clade I (Fig. 5), then M-shaped frames evolved convergently a third time. New sources of data are necessary to clarify the issue.

The frames of *Lepocinclis buetschlii*, *E. acus*, and clade J are similar in possessing a very subtle median depression (Mignot 1965; Bricheux and Brugerolle 1986, 1987; Leander and Farmer 2001a,b), and, accordingly, these taxa clustered together in the analysis of morphological data. The combined and separate molecular analyses, however, provide results that conflict with the morphological tree, so inferring the evolution of these frames with confidence is currently not possible.

S-shaped frames (state 16-1, Table 2) are inferred to be

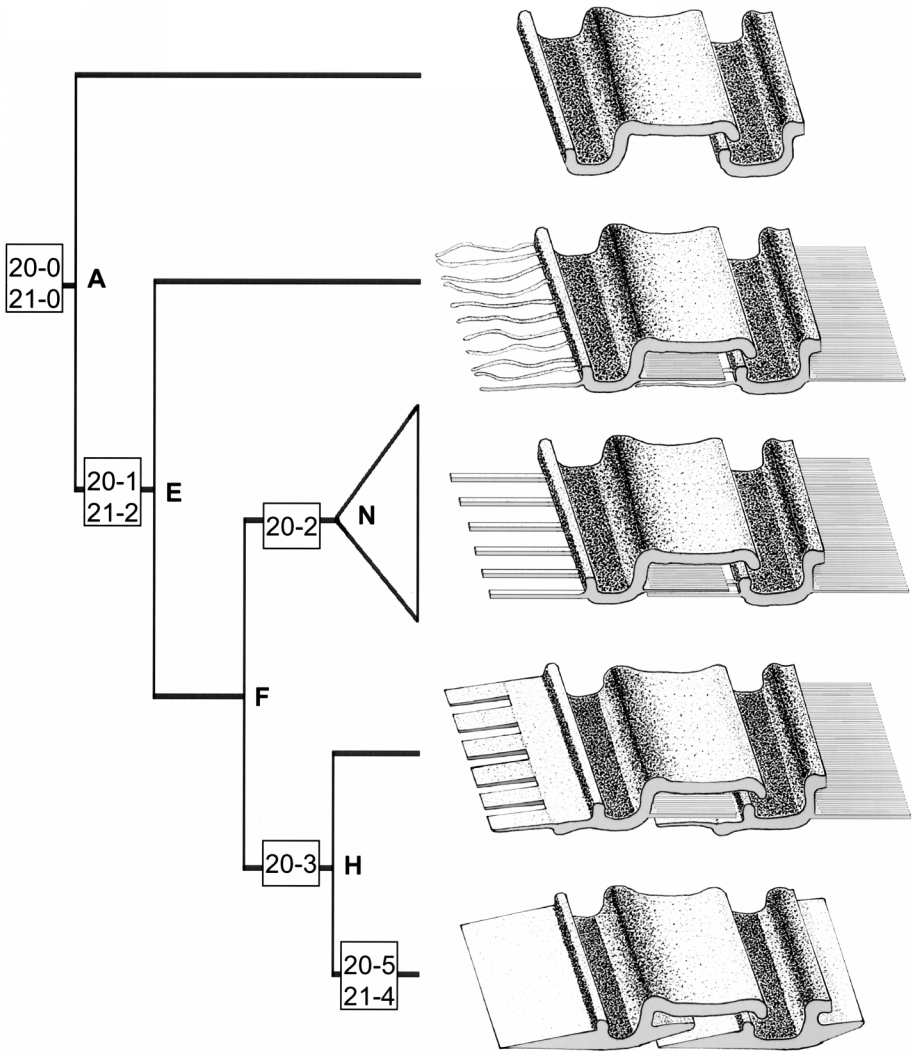

FIG. 10. Diagram illustrating the evolution of strip projections. Letters at the nodes correspond to Figure 6 and numbers separated by dashes denote the relevant character states (Tables 2, 3). The arches of the right strips have been removed for clarity. Strip projections started out delicate and became more robust at least two times independently within clade F. Other lineages with delicate projections that diverged between clades N and H have been omitted (see Fig. 6).

the ancestral state for clade B. *Peranema trichophorum* possesses plateau-shaped frames (state 16-2, Table 2) and a gradual transition between the heel and the arch (Fig. 2A); this is a combination of features that bridges the S-shaped frames of *D. proteus* (Mignot 1965) with the keeled frames of clade D (Leander and Farmer 2001b). In other words, plateau-shaped frames are inferred to be the ancestral state for clade C and the presence of distinct keels (state 18-1, Table 2; Fig. 2B, D) unifies clade D. These transformations are complicated by independent reversals from plateau-shaped frames to S-shaped frames in *E. mutabilis* and *E. myxocylindracea* (Fig. 6).

Even though homoplasy played a significant role in the evolution of frames, some frame-based characters provide robust evidence for phylogenetic relationships. For example, the presence of minor grooves (state 17-1, Table 2), which are modifications of the median depressions in the M-shaped frames of clade H, is a good synapomorphy for clade K (Leander and Farmer 2001b; Fig. 6). It has been suggested that the origin of minor grooves was associated with a symbiosis with rod-shaped epibiotic bacteria (Leander and Farmer 2000b).

The Evolution of Strip Projections

Our results show that strip projections (characters 20 and 21, Table 2) evolved after the origin of plastids in the common ancestor of clade E (Figs. 6, 8, 10). Both prearticular strip projections in the form of delicate strands and postarticular projections in the form of a delicate indented plate arose before the more robust states for these characters (Fig. 10). It is relevant to consider that euglenoid movement is most pronounced in taxa possessing helical pellicles that entirely lack strip projections, such as *D. proteus* and *P. trichophorum*, and in the phototrophic taxa that diverge near the origin of clade E, namely *E. pertyi* and *E. mutabilis*. The

degree of euglenoid movement is markedly lower within clade F, wherein the prearticular projections became more robust in clades H and N independently (Fig. 10). The taxa in clade H possess either semiplastic or rigid pellicles associated with toothlike (states 20-3 and 21-3, Table 2) and platelike (states 20-5 and 21-4, Table 2) strip projections. The parsimony analyses suggest that the platelike projections of clade K were derived from toothlike projections, and the basal plate in the latter provides supporting evidence for this hypothesis (Figs. 6, 10). In clade N, the prearticular projections became more robust as linear threads (state 20-2, Table 2; Fig. 10). The taxa in clade I possess rigid pellicles with robust dove-tailed prearticular projections (state 20-4, Table 2; Leander and Farmer 2001a); however, whether this state is a modification of the toothlike projections of clade H or a third example of parallel evolution remains to be clarified.

Despite contrary opinions (Chu 1947; Suzaki and Williamson 1986b), there does appear to be a correlation between the presence and robustness of strip projections and a more limited degree of euglenoid movement (Dragos et al. 1997). Robust strip projections (e.g., platelike) are also associated with large cell size as has been noted already for clade K. Nonetheless, the prior correlation leads us to hypothesize that strip projections evolved as the structural means for either slowing or, in some taxa, completely halting euglenoid movement. This view assumes that euglenoid movement decreased fitness in the ancestral taxa that abandoned eukaryotrophy for a phototrophic mode of life. Studies on the orientation of the delicate strip projections of *A. longa* during contracted and relaxed stages of euglenoid movement lend evidence to the view that projections actually resist the displacement of sliding strips (Suzaki and Williamson 1986a). If we view the main disadvantage of euglenoid movement in phototrophs as being energetically unnecessary, then evolution of strip projections is somewhat paradoxical in that cellular resources need to be consumed to build projections that presumably minimize the consumption of cellular resources involved with euglenoid movement. We could therefore conclude that the cost of building static strip projections is less than the cost of the dynamic process of euglenoid movement.

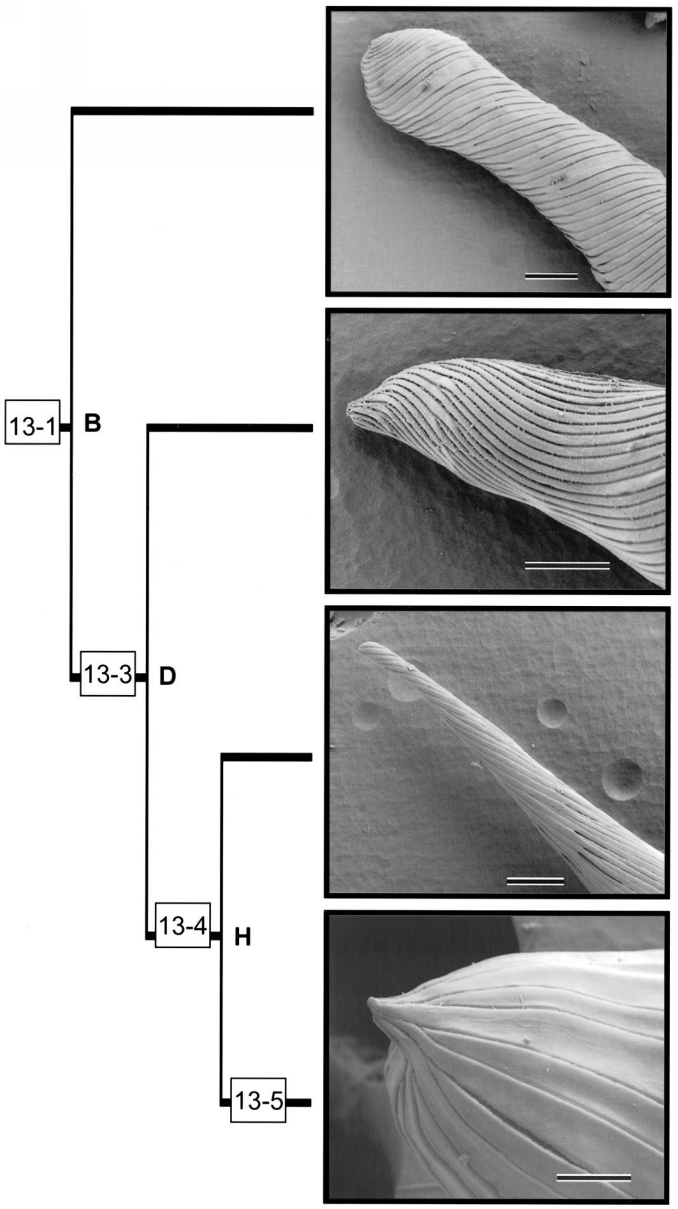

FIG. 11. Diagram illustrating the evolution of posterior tip morphology. Letters at the nodes correspond to Figure 6 and numbers separated by dashes denote the relevant character states (Tables 2, 3). The scanning electron micrographs were taken from the following taxa, from top to bottom: *Distigma proteus* (bar = 2.5 μm), *Euglena stellata* (bar = 2.5 μm), *Euglena acus* (bar = 2.5 μm), and *Phacus oscillans* (bar = 2 μm). Most of the taxa in clade H possess sharp posterior tips (13-4, Table 2; Fig. 6).

The Evolution of Posterior Tip Morphology

For euglenids with helical pellicles, the morphology of the posterior tip takes on four basic states with the following polarity: rounded → conical → sharply pointed → stubby (Figs. 6, 11). In accordance with the synthetic tree, the ancestral state for clade B is rounded (state 13-1, Table 2), the ancestral state for clade D is conical (state 13-3, Table 2), and the ancestral state for clade H is sharply pointed (state 13-4, Table 2; Figs. 6, 11). The taxa within clade H possessing stubby posterior tips (state 13-5, Table 2), namely clade J and *L. buetschlii*, are inferred to have evolved from taxa with sharply pointed posterior tips (Fig. 11).

Variation in posterior tip morphology may have evolved by subtle changes in mechanisms associated with cytokinesis that are analogous to the phenomenon of rotokinesis (spinning movements of a daughter cell that facilitates separation during late cytokinesis) in dividing *Tetrahymena* (Brown et al. 1999; Leander and Farmer 2001a). As the longitudinal cleavage furrow migrates posteriorly during cytokinesis in euglenids, each daughter cell rotates around its own longitudinal axis in the same direction, which is either clockwise or counterclockwise depending on the orientation of the strips in the interphase cell (Sommer and Blum 1965; Hofmann and Bouck 1976; Bouck and Ngo 1996; Fig. 12A). When the cleavage furrow reaches the posterior tip, two events take place. First, the daughter cells remain connected but the anterior ends have migrated away from one another so that the two cells now share the same longitudinal axis, where the

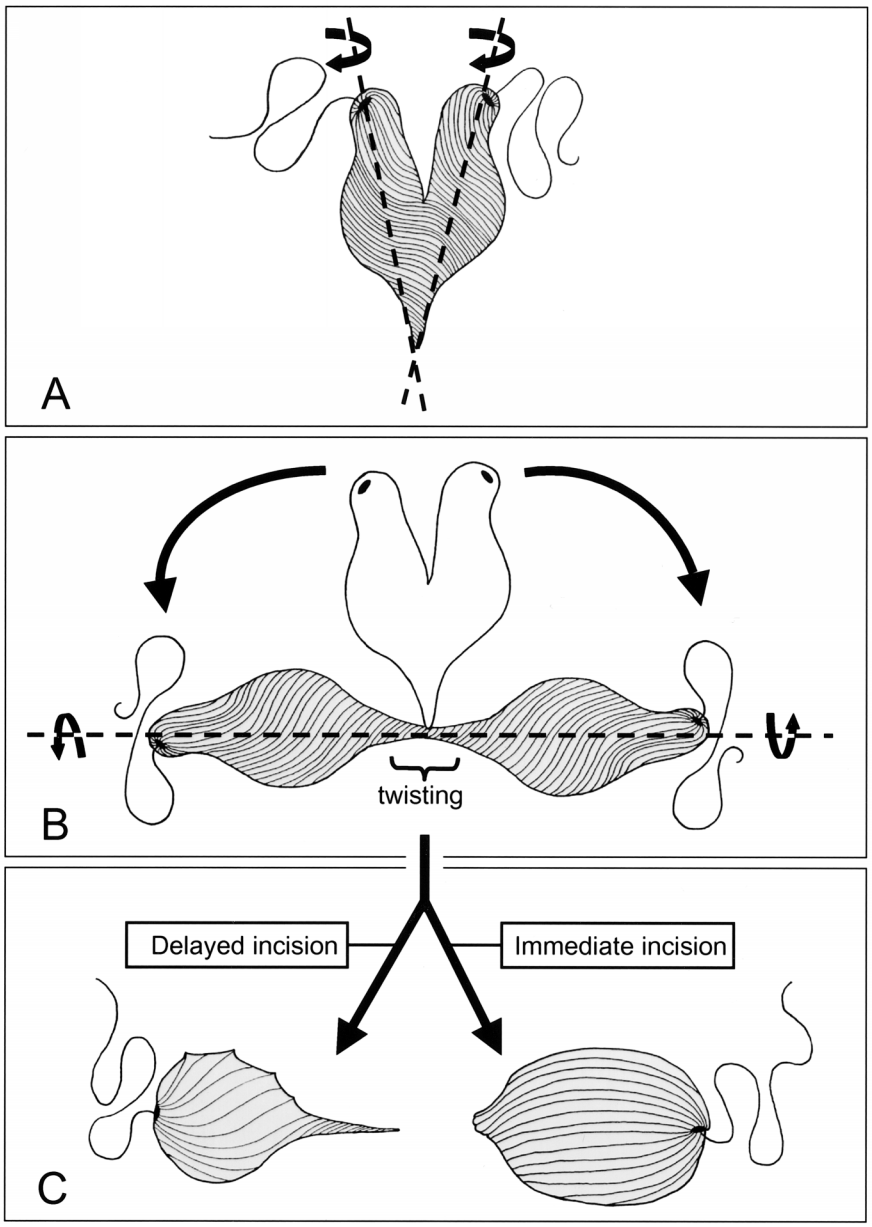

FIG. 12. The hypothetical mechanisms involved in the evolution of posterior tip morphology in euglenids. (A) As the cleavage furrow migrates posteriorly during cytokinesis, each daughter cell rotates slowly in the same direction along their longitudinal axes. (B) After the anterior ends of each daughter cell have migrated away from each other, the two cells can now spin in opposite directions along the same longitudinal axis. This causes twisting of the posterior ends of each cell. (C) The morphology of the posterior end depends on cell rigidity and the timing of a putative incision mechanism. A delayed incision event causes sharp posterior ends (left cell) and an immediate incision event causes stubby posterior ends (right cell).

anterior ends of each daughter cell are at opposite poles (Sommer and Blum 1965; Fig. 12B). Because each daughter cell can maintain the same rotational movement via distinct flagellar beat patterns, the two cells may now spin in opposite directions (Fig. 12B). This produces pellicular twisting near the junction between the daughters. Second, the amount of time that twisting occurs at the junction between the daughter cells depends on a putative incision mechanism. The longer the two cells remain attached to one another before incision, the more twisted and drawn out the posterior end of the cell may become. The amount of twisting would also depend on the rate that each daughter cell spins. Taxa with rigid pellicles near the posterior end would tend to retain the morphology of the posterior end caused by these (possibly genetically controlled) events, whereas taxa with relatively plastic pellicles would tend to possess posterior ends that are less sharp because of cytoskeletal elasticity.

With respect to the rigid taxa we examined, two extreme states for the morphology of the posterior end were observed, namely sharply pointed and stubby (Figs. 3E, 12). We infer that the taxa with sharp posterior ends (e.g., *E. acus*, *E. spirogyra*, and *E. tripteris*) incurred relatively more twisting via

a delayed incision event (Fig. 12C). The taxa with stubby posterior ends (e.g., clade J) are inferred to have sustained less twisting, where the rate of spinning was nil and the incision event happened quickly once the cleavage furrow reached the posterior end (Fig. 12C). Some rigid taxa (e.g., *P. curvatus* and *P. hamitus*; Tell and Conforti 1986) have drawn out posterior ends that are kinked or curved. This may be a simple consequence of connected daughter cells that do not exactly align onto the same longitudinal axis during the twisting stage (Fig. 12B).

Summary and Conclusions

Here we attempted to cladistically integrate a large morphological dataset from single-celled organisms into a molecular context to document novel cases of character evolution. The results demonstrate some remarkable trends in the evolution of morphological features in euglenids that can only be observed with the assistance of electron microscopy. For instance, the number of strips around the cell periphery increased significantly along the lineage leading to the ancestor of phototrophs, but the number of strips changed idiosyncratically within the group. The increase in strip number is associated with euglenoid movement and the adoption of eukaryotrophic modes of feeding, which preceded the origin of euglenid plastids. One mechanism for increasing the origin of pellicle strips is by permanent strip-doubling events that may occur when a cell prepares its cytoskeleton for division but fails to undergo cytokinesis. Once euglenids acquired plastids and abandoned eukaryotrophy, the number of strips decreased along independent lineages and the pellicle became more rigid in the group as a whole. Moreover, strip projections first emerged within phototrophs and became particularly robust in semiplastic and rigid taxa. The presence of strip projections within phototrophs is inferred to be a mechanism for preventing euglenoid movement, where cell plasticity is presumed to be an expendable cytoskeletal property in euglenids capable of photosynthesis.

A pattern of strip reduction consisting of whorls on the surface of euglenid cells marks the origin of phototrophy, which is useful for interpreting the biology of acritarch fossils. The study showed that linear and pseudolinear patterns of strip reduction are ancestral to the exponential pattern indicating that taxa like *E. pertyi* and *E. mutabilis* are among the earliest diverging phototrophs. The specific patterns of terminating strips are more involved than optimal packing under the constraints of posterior tip morphology, the number of strips, the width of the strips, and the size of the cell. Morphology of the cell posterior tip within euglenids possessing helical pellicles had the following polarity: rounded $\rightarrow$ conical $\rightarrow$ sharp $\rightarrow$ stubby. A putative mechanism was proposed to account for this diversity. We hope that these descriptions of specific pellicle characters in euglenids will stimulate research on the processes controlling their morphology. A better understanding of euglenid biodiversity and cell biology should significantly enhance our understanding of natural history, particular with respect to endosymbiosis and the origin of the eukaryotic cell.

Acknowledgments

Financial support was provided by the National Science Foundations Partnerships for Enhancing Expertise in Taxonomy (grant no. DEB 4-21348). The authors wish to acknowledge R. E. Triemer for providing us with a wild sample containing *Euglena oxyuris*. We are grateful to P. J. P. Brown and J. P. Shields for technical support. We also thank C. A. Leander and D. Porter for providing laboratory space and assistance with the generation of DNA sequences. The editorial comments from J. V. McHugh and two anonymous reviewers provided new insight and significantly enhanced the clarity of the manuscript.

Literature Cited

Angeler, D. G., A. N. Müllner, and M. Schagerl. 1999. Comparative ultrastructure of the cytoskeleton and nucleus of *Distigma* (Euglenozoa). Eur. J. Protistol. 35:309–318.

Baldauf, S. L., A. J. Roger, I. Wenk-Siefert, and W. F. Doolittle. 2000. A kingdom-level phylogeny of eukaryotes based on combined protein data. Science 290:972–976.

Bouck, G. B., and H. Ngo. 1996. Cortical structure and function in euglenoids with reference to trypanosomes, ciliates, and dinoflagellates. Int. Rev. Cytol. 169:267–318.

Bricheux, G., and G. Brugerolle. 1986. The membrane cytoskeleton complex of euglenids. I. Biochemical and immunological characterization of epiplasmic proteins in *Euglena acus*. Europ. J. Cell Biol. 40:150–159.

———. 1987. The pellicular complex of euglenoids. II. A biochemical and immunological comparative study of major epiplasmic proteins. Protoplasma 140:43–54.

Brown, J. M., C. Hardin, and J. Gaertig. 1999. Rotokinesis, a novel phenomenon of cell locomotion-assisted cytokinesis in the ciliate *Tetrahymena thermophila*. Cell Biol. Int. 23:841–848.

Bull, J. J., J. P. Huelsenbeck, C. W. Cunningham, D. L. Swofford, and P. J. Waddell. 1993. Partitioning and combining data in phylogenetic analysis. Syst. Biol. 42:384–397.

Chippindale, P. T., and J. J. Weins. 1994. Weighting, partitioning, and combining characters in phylogenetic analysis. Syst. Biol. 43:278–287.

Chu, S. P. 1947. Contribution to our knowledge of the genus *Euglena*. Sinensia 17:75–136.

Dawson, N. S., and P. L. Walne. 1991. Structural characterization of *Eutreptia pertyi* (Euglenophyta), I. General description. Phycologia 30:287–302.

de Queiroz, A. 1993. For consensus (sometimes). Syst. Biol. 42: 368–372.

Dragos, N., L. S. Péterfi, and C. Popescu. 1997. Comparative fine structure of pellicular cytoskeleton in *Euglena* Ehrenberg. Arch. Protistenkd. 148:277–285.

Dubreuil, R. R., and G. B. Bouck. 1985. The membrane skeleton of a unicellular organism consists of bridged, articulating strips. J. Cell Biol. 101:1884–1896.

Elwood, H. J., G. J. Olsen, and M. L. Sogin. 1985. The small-subunit ribosomal RNA gene sequences from hypotrichous ciliates *Oxytricha nova* and *Stylonychia pustulata*. Mol. Biol. Evol. 2:399–410.

Eriksson, T. 1998. AutoDecay. Ver. 4.0. Program distributed by the author. Bergius Foundation, Royal Swedish Academy of Sciences, Stockholm.

Felsenstein, J. 1985. Confidence limits on phylogenies: an approach using the bootstrap. Evolution 39:783–791.

Gallo, J. M., and J. Shrével. 1982. Euglenoid movement in *Distigma proteus*. I. Cortical rotational motion. Biol. Cell 44:139–148.

Gibbs, S. P. 1978. The chloroplasts of *Euglena* may have evolved from symbiotic green algae. Can. J. Bot. 56:2883–2889.

Goff, L., and D. Moon. 1993. PCR amplification of nuclear and plastid genes from algal herbarium specimens and algal spores. J. Phycol. 29:381–384.

Gould, S. J. 1988. Trends as changes in variance: a new slant on

progress and directionality in evolution. J. Paleontol. 62: 319–329.
———. 1990. Speciation and sorting as the source of evolutionary trends, or ''Things are seldom what they seem.'' Pp. 3–27 *in* K. J. McNamara, ed. Evolutionary trends. Univ. of Arizona Press, Tucson, AZ.
———. 1996. Full house. Harmony Books, New York.
Gould, S. J., and E. S. Vrba. 1982. Exaptation—a missing term in the science of form. Paleobiology 8:4–15.
Gray, J., and A. J. Boucot. 1989. Is *Moyeria* a euglenoid? Lethaia 22:447–456.
Gray, M. W., B. F. Lang, R. Cedergren, G. B. Golding, C. Lemieux, D. Sankoff, M. Turmel, N. Brossard, E. Delage, T. G. Littlejohn, I. Plante, P. Rioux, D. Saint-Louis, Y. Zhu, and G. Burger. 1998. Genome structure and gene content in protist mitochondrial DNAs. Nucleic Acids Res. 26:865–878.
Hausmann, K. 1978. Extrusive organelles in protists. Int. Rev. Cytol. 52:197–268.
Hausmann, K., and J. P. Mignot. 1977. Untersuchungen an den mucocysten von *Euglena splendens* Dangeard 1901. Protistologica 13:213–217.
Hilenski, L. L., and P. L. Walne. 1983. Ultrastructure of mucocysts in *Peranema trichophorum* (Euglenophyceae). J. Protozool. 30: 491–496.
Hofmann, C., and G. B. Bouck. 1976. Immunological and structural evidence for patterned intussusceptive surface growth in a unicellular organism. J. Cell Biol. 69:693–715.
Huelsenbeck, J. P., J. J. Bull, and C. W. Cunningham. 1996. Combining data in phylogenetic analysis. Trends Ecol. Evol. 11: 152–158.
Keeling, P. J., J. A. Deane, and G. I. McFaddan. 1998. The phylogenetic position of alpha- and beta-tubulins from the *Chlorarachnion* host and *Cercomonas* (Cercozoa). J. Eukaryot. Microbiol. 45:561–570.
Kirk, J. T. O., and B. E. Juniper. 1964. The fine structure of the pellicle of *Euglena gracilis*. J. R. Microsc. Soc. 82:205–210.
Kluge, A. G. 1989. A concern for evidence and a phylogenetic hypothesis of relationships among *Epicrates* (Boidae, Serpentes). Syst. Zool. 38:7–25.
———. 1998. Total evidence or taxonomic congruence: cladistics or consensus classification. Cladistics 14:151–158.
Kluge, A. G., and A. J. Wolf. 1993. Cladistics: What's in a word? Cladistics 9:183–199.
Lanyon, S. M. 1993. Phylogenetic frameworks: towards a firmer foundation for the comparative approach. Biol. J. Linn. Soc. 49: 45–61.
Leander, B. S., and M. A. Farmer. 2000a. Comparative morphology of the euglenid pellicle. I. Patterns of strips and pores. J. Eukaryot. Microbiol. 47:469–479.
———. 2000b. Epibiotic bacteria and a novel pattern of strip reduction on the pellicle of *Euglena helicoideus* (Bernard) Lemmermann. Europ. J. Protistol. 36:405–413.
———. 2001a. The evolution of *Phacus* (Euglenozoa) as inferred from pellicle morphology and SSU rDNA. J. Phycol. 37:1–17.
———. 2001b. Comparative morphology of the euglenid pellicle. II. Diversity of strip substructure. J. Eukaryot. Microbiol. 48: 202–217.
Leander, B. S., R. E. Triemer, and M. A. Farmer. 2001. Character evolution in heterotrophic euglenids. Europ. J. Protistol. 37: 337–356.
Leedale, G. F. 1964. Pellicle structure in *Euglena*. Brit. Phycol. Bull. 2:291–306.
Lefort-Tran, M., M. H. Bre, J. L. Ranck, and M. Pouphile. 1980. *Euglena* plasma membrane during normal and vitamin B_{12} starvation growth. J. Cell Sci. 41:245–261.
Linton, E. W., D. Hittner, C. Lewandowski, T. Auld, and R. E. Triemer. 1999. A molecular study of euglenoid phylogeny using small subunit rDNA. J. Eukaryot. Microbiol. 46:217–223.
Linton, E. W., A. Nudelman, V. Conforti, and R. E. Triemer. 2000. A molecular analysis of the genus *Euglena* (Euglenophyta) using SSU rDNA. J. Phycol. 36:740–746.
Mignot, J. P. 1965. Ultrastructure des eugléniens, I. Étude de la cuticle chez différentes espéces. Protistologica 1:5–15.
Mignot, J. P., and R. Hovasse. 1973. Nouvelle contribution à la connaissance des trichocystes: les organites grillages d'*Entosiphon sulcatum* (Flagellata, Euglenida). Protistologica 9: 373–391.
Mignot, J. P., G. Brugerolle, and G. Bricheux. 1987. Intercalary strip development and dividing cell morphogenesis in the euglenid *Cyclidiopsis acus*. Protoplasma 139:51–65.
Milanowski, R., B. Zakryś, and J. Kwiatowski. 2001. Chloroplast small subunit rRNA genes reveal the polyphyletic nature of the genus *Euglena* Ehrenberg. Int. J. Syst. Evol. Microbiol. 51: 773–781.
Miyamoto, M. M., and W. M. Fitch. 1995. Testing species phylogenies and phylogenetic methods with congruence. Syst. Biol. 44:64–76.
Montegut-Felkner, A. E., and R. E. Triemer. 1997. Phylogenetic relationships of selected euglenoid genera based on morphological and molecular data. J. Phycol. 33:512–519.
Müllner, A. N., D. G. Angeler, R. Samuel, E. W. Linton, and R. E. Triemer. 2001. Phylogenetic analysis of phagotrophic, phototrophic and osmotrophic euglenoids by using the nuclear 18S rDNA sequence. Int. J. Syst. Evol. Microbiol. 51:783–791.
Nisbet, B. 1974. An ultrastructural study of the feeding apparatus of *Peranema trichophorum*. J. Protozool. 21:39–48.
Petersen-Mahrt, S. K. 1997. The surface complex of *Euglena gracilis*. Ph.D. diss., Lund University, Lund, Sweden. Available from Lund University, Section of Plant Physiology, accession number LUNBDS/nbfb-1032/1-102.
Preisfeld, A., I. Busse, M. Klingberg, S. Talke, and H. G. Ruppel. 2000. Phylogenetic analysis of various euglenoid taxa (Euglenozoa) based on 18S rDNA sequence data. J. Phycol. 36: 220–226.
Preisfeld, A., S. Berger, I. Busse, S. Liller, and H. G. Ruppel. 2001. Phlogenetic position and inter-relationships of the osmotrophic euglenids based on SSU rDNA data, with emphasis on the Rhabdomonadales. Int. J. Syst. Evol. Microbiol. 51:751–758.
Rambaut, A. 1996. Sequence alignment editor. Ver. 1.0 alpha 1. Program available via http://evolve.zoo.ox.ac.uk/Se-Al/Se-Al.html.
Schwelitz, F. D., W. R. Evans, H. H. Mollenhaur, and R. A. Dilley. 1970. The fine structure of the pellicle of *Euglena gracilis* as revealed by freeze-etching. Protoplasma 69:341–349.
Sogin, M. L. 1997. History assignment: When was the mitochondrion founded? Curr. Opin. Genet. Dev. 7:792–799.
Sommer, J. R. 1965. The ultrastructure of the pellicle complex of *Euglena gracilis*. J. Cell Biol. 24:253–257.
Sommer, J. R., and J. J. Blum. 1965. Cell division in *Astasia longa*. Exp. Cell Res. 39:504–527.
Starr, R. C., and J. A. Zeikus. 1993. UTEX: the culture collection of algae at the University of Texas at Austin, 1993 list of cultures. J. Phycol. 29:1–106.
Suzaki, T., and R. E. Williamson. 1985. Euglenoid movement in *Euglena fusca*: evidence for sliding between pellicular strips. Protoplasma 124:137–146.
———. 1986a. Ultrastructure and sliding of pellicular structures during euglenoid movement in *Astasia longa* Pringsheim (Sarcomastigophora, Euglenida). J. Protozool. 33:179–184.
———. 1986b. Pellicular ultrastructure and euglenoid movements in *Euglena ehrenbergii* Klebs and *Euglena oxyuris* Schmarda. J. Protozool. 33:165–171.
Swofford, D. L. 1999. PAUP*: phylogenetic analysis using parsimony (and other methods). Ver. 4.0. Sinauer Associates, Sunderland, MA.
Tell, G., and V. Conforti. 1986. Euglenophyta pigmentadas de la Argentina. Bibliotheca Phycologica, Berlin.
Thompson, M. D., D. W. Copertino, E. Thompson, M. R. Favreau, and R. B. Hallick. 1995. Evidence for the late origin of introns in chloroplast genes from an evolutionary analysis of the genus *Euglena*. Nucleic Acids Res. 23:4745–4752.
Triemer, R. E. 1997. Feeding in *Peranema trichophorum* Revisited (Euglenophyta). J. Phycol. 33:649–654.
Van de Peer, Y., E. Robbrecht, S. de Hoog, A. Caers, P. De Rijk, and R. De Wachter. 1999. Database on the structure of small subunit ribosomal RNA. Nucleic Acids Res. 27:179–183.
Wiens, J. J. 1998. Combining datasets with different phylogenetic histories. Syst. Biol. 47:568–581.

Corresponding Editor: M. Riley